RESEARCH LETTER

AMERICAN JOURNAL OF medical genetics PART A

Prenatal Diagnosis of Costello Syndrome Using 3D Ultrasonography Amniocentesis Confirmation of the Rare HRAS Mutation G12D

Hideo Kuniba,[1,2]* Ritsuko K. Pooh,[3] Kensaku Sasaki,[4] Osamu Shimokawa,[4] Naoki Harada,[4] Tatsuro Kondoh,[2,5] Masanori Egashira,[2] Hiroyuki Moriuchi,[2] Koh-ichiro Yoshiura,[1] and Norio Niikawa[1,6]

[1]Department of Human Genetics, Nagasaki University Graduate School of Biomedical Sciences, Nagasaki, Japan

[2]Department of Pediatrics, Nagasaki University Graduate School of Biomedical Sciences, Nagasaki, Japan

[3]CRIFM Clinical Research Institute of Fetal Medicine PMC, Osaka, Japan

[4]Kyushu Medical Science Nagasaki Laboratory (KMS), Nagasaki, Japan

[5]Department of Clinical Genetics, Misakae-no-sono Mutsumi, Institute for Severe Intellectual/Motor Disabled Persons, Isahaya, Japan

[6]Research Institute of Personalized Health Sciences, Health Sciences University of Hokkaido, Tobetsu, Japan

Received 8 February 2008; Accepted 12 March 2008

TO THE EDITOR:

Costello syndrome (CS, OMIM #218040) is a rare disorder with a distinctive facial appearance, prenatal overgrowth, poor postnatal growth, loose skin of the hands and feet, characteristic hand position, developmental delay, papillomata, cardiac abnormalities, and tumor predisposition. *HRAS* is the only gene currently known to be causative for CS [Aoki et al., 2005; Nava et al., 2007; Rauen, 2007]. Almost all of the mutations of the *HRAS* gene in CS patients which have been reported subsequently have been diagnosed after infancy [Estep et al., 2006; Gripp et al., 2006; Kerr et al., 2006; Schulz et al., 2008] except for patients presenting with severe neonatal manifestation of CS [Lo et al., 2008]. We report on the first patient with prenatally diagnosed CS dues to the rare c.35G > A, p.G12D *HRAS* mutation.

A 31-year-old G2P1 woman was referred at 23 weeks of gestation for ultrasonography which showed polyhydramios, good fetal movement, and overgrowth with estimated body weight 1,300 g (+5.3 SD using a Japanese fetal growth curve). There was no pleural effusion, ascites or subcutaneous edema. Craniofacial features included large head (+3.0 SD), pointed chin, full cheeks, wide nasal bridge, and low-set ears (Fig. 1A), but no macroglossia, omphalocele, hydrocephalus, or brain anomalies. The size of the abdomen was equivalent to that of a fetus at 28–31 weeks gestation. The fetal stomach could not be identified. Hepatomegaly was detected, but the other visceral organs were normal. The extremities were normal in length without deformity, although the wrists were deviated laterally.

Cytogenetic and molecular analyses were performed after obtaining informed consent from parents. Standard chromosomes analysis by amniocentesis showed normal karyotype: 46,XY. The deletion of *NSD1* responsible for Sotos syndrome was not detected by fluorescence in situ hybridization (data not shown). By the time CS was suspected, the volume of amniotic fluid was only 1.8 ml which was frozen and stored in the clinic. To perform molecular diagnosis for CS, DNA was extracted with QIAvac vacuum manifold (Qiagen, Chatsworth, CA) from the specimen, and whole genome amplification was carried out with GenomePlex Whole Genome Amplification Kit (Sigma–Aldrich, St. Louis, MO), according to the manufacture's instructions. In this procedure, 3 μg of DNA was obtained. All *HRAS* coding exons and their flanking intronic sequences were analyzed by direct sequencing on an ABI 3100 automated sequencer (Applied Biosystems, Foster City, CA), and a rare missense mutation was found, that is, c.35G > A, p.G12D (Fig. 1B).

How to Cite this Article:
Kuniba H, Pooh RK, Sasaki K, Shimokawa O, Harada N, Kondoh T, Egashira M, Moriuchi H, Yoshiura K, Niikawa N. 2009. Prenatal diagnosis of Costello syndrome using 3D ultrasonography amniocentesis confirmation of the rare HRAS mutation G12D.
Am J Med Genet Part A 149A:785–787.

*Correspondence to:
Dr. Hideo Kuniba, Department of Pediatrics, Nagasaki University Graduate School of Biomedical Sciences, Sakamoto 1-12-4, Nagasaki 852-8523, Japan. E-mail: kuniba03@nifty.com

Published online 18 July 2008 in Wiley InterScience (www.interscience.wiley.com)
DOI 10.1002/ajmg.a.32335

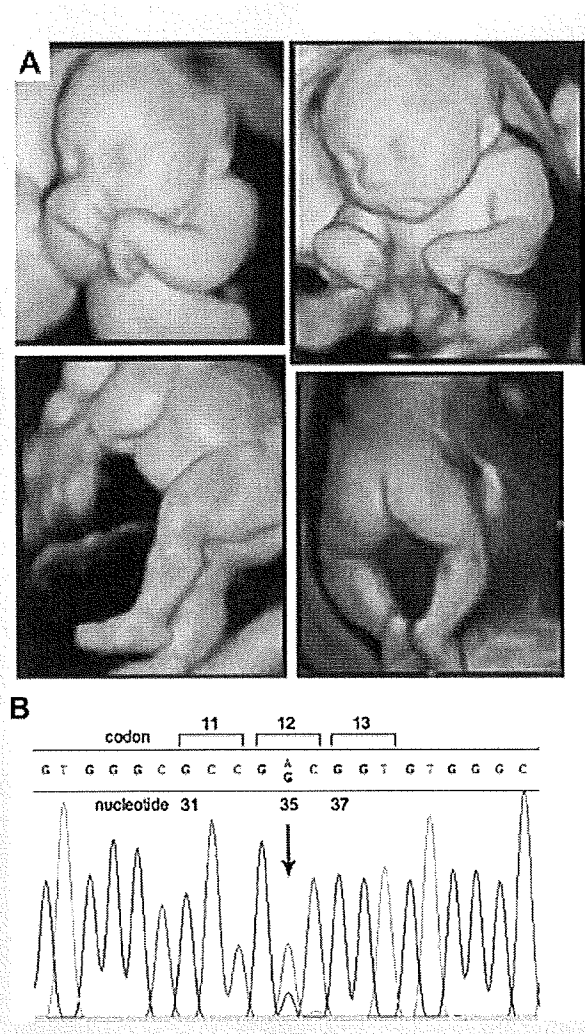

FIG. 1. A: Three-dimensional ultrasound images of the fetus at 24 weeks of gestation with overgrowth and so-called "coarse face". Note his left hand presenting ulnar deviation and flexion of the wrist. B: Electropherogram of *HRAS* showing missense mutation at codon 12, c.35G > A, p.G12D. [Color figure can be viewed in the online issue, which is available at www.interscience.wiley.com.]

The mother had been transported to a pediatric hospital after the fetal evaluation, and the fetus subsequently developed pleural effusion and deteriorated. He was born at 31 weeks gestation via cesarean. He weighed 2,926 g (+4.2 SD) and developed respiratory failure, severe hypoglycemia, cardiac hypertrophy and renal failure. Although he was treated in neonatal intensive care unit, he died soon after birth due to multiple organ failures. Permission for autopsy was not granted. We were unable to study the parental origin [Sol-Church et al., 2006; Zampino et al., 2007] because DNA samples from the mother and his 33-year-old father had not been obtained.

Prenatal overgrowth and polyhydramios were prominent in this case. Dysmorphic facial features and flexion of the wrist, imaged with striking clarity by three-dimensional (3D) ultrasonography led us to a clinical diagnosis of CS. Prenatal overgrowth syndromes include relatively few conditions, that is, Sotos syndrome, Simpson–Golabi–Behmel syndrome, Beckwith–Wiedemann syndrome, and CS. The presence of polyhydramios which occurs in over 90% of pregnancies with CS, supported by the 3D ultrasonographic imaging of facial features (broad nose, puffy cheeks, so-called "coarse" face, pointed chin, and flexion of the wrist) made the diagnosis likely. Three-dimensional ultrasonography is clearly more beneficial than two-dimensional (2D) ultrasonography in a diagnosis of genetic syndromes, since we can see overall fetal image of malformation which we hardly get with conventional 2D ultrasonography [Lee and Simpson, 2007]. The phenotype of Noonan syndrome often overlaps with that of CS, and the prenatal findings of Noonan syndrome, polyhydramnios and so-called "coarse face" in a fetus with the T854C mutation in the *PTPN11* gene, have been reported [Levaillant et al., 2006], although that fetus with Noonan syndrome did not develop overgrowth.

CS was diagnosed clinically in the prenatal period in monozygotic twins who died 57 days of life after birth at 30 weeks of gestation due to respiratory failure [Van den Bosch et al., 2002]. Molecular diagnosis was not available. Neonatal deaths in two patients with CS confirmed by molecular diagnosis of G12D *HRAS* mutation were reported by Lo et al. [2008]. One patient was born at 36 weeks gestation weighing 2,950 g developed hypoglycemia, persistent and severe jaundice, persistent respiratory distress with tracheomalacia, bronchomalacia and chylothorax. The baby also had clenched hands, atrial septal defect, paroxysmal multifocal atrial tachycardia, pulmonary lymphangiectasia, and renal failure. She died at age 3 months due to respiratory failure. The other patient was a girl born at 37 weeks gestation weighing 3,115 g had hypoglycemia, rhizomelic limb shortening and flexion contractures at the wrist, hypertrophic cardiomyopathy, dysplasic pulmonary valve, atrial fibrillation, cardiac failure and persistent hyponatremia due to renal sodium leakage. She became ventilator dependent and died at 3 months of age from sepsis and renal failure. Both had pregnancies complicated by polyhydramios. Lo et al. [2008] suggested that differences in activating potential of G12D mutations in *HRAS* gene may result in severe manifestations, such as hypoglycemia, renal abnormalities, severe early cardiomyopathy, and congenital respiratory abnormalities, which result in multiple organ failure.

We believe this is the first case of prenatally diagnosed CS confirmed with molecular genetic analysis with a G12D mutation in *HRAS* gene. The mutation was not observed in previous natural history studies of CS, perhaps because of the rarity of the mutation and the fact that the patients die in early infancy. Our findings contribute to the natural history of this mutation which includes a severe clinical course. If prenatal ultrasonographic findings show both polyhydramnios and overgrowth, CS should be considered despite its rarity. Molecular diagnosis should be offered in the perinatal period without hesitation.

ACKNOWLEDGMENTS

We are grateful to the family for their participation in this research. We thank Dr. Shoko Miura for her helpful comments.

REFERENCES

Aoki Y, Niihori T, Kawame H, Kurosawa K, Ohashi H, Tanaka Y, Filocamo M, Kato K, Suzuki Y, Kure S, Matsubara Y. 2005. Germline mutations in HRAS proto-oncogene cause Costello syndrome. Nat Genet 37: 1038–1040.

Estep AL, Tidyman WE, Teitell MA, Cotter PD, Rauen KA. 2006. HRAS mutations in Costello syndrome: Detection of constitutional activating mutations in codon 12 and 13 and loss of wild-type allele in malignancy. Am J Med Genet Part A 140A:8–16.

Gripp KW, Lin AE, Stabley DL, Nicholson L, Scott CI Jr, Doyle D, Aoki Y, Matsubara Y, Zackai EH, Lapunzina P, Gonzalez-Meneses A, Holbrook J, Agresta CA, Gonzalez IL, Sol-Church K. 2006. HRAS mutation analysis in Costello syndrome: Genotype and phenotype correlation. Am J Med Genet Part A 140A:1–7.

Kerr B, Delrue MA, Sigaudy S, Perveen R, Marche M, Burgelin I, Stef M, Tang B, Eden OB, O'Sullivan J, De Sandre-Giovannoli A, Reardon W, Brewer C, Bennett C, Quarell O, M'Cann E, Donnai D, Stewart F, Hennekam R, Cave H, Verloes A, Philip N, Lacombe D, Levy N, Arveiler B, Black G. 2006. Genotype-phenotype correlation in Costello syndrome: HRAS mutation analysis in 43 cases. J Med Genet 43:401–405.

Lee YM, Simpson LL. 2007. Major fetal structural malformations: The role of new imaging modalities. Am J Med Genet Part C Semin Med Genet 145C:33–44.

Levaillant JM, Gerard-Blanluet M, Holder-Espinasse M, Valat-Rigot AS, Devisme L, Cave H, Manouvrier-Hanu S. 2006. Prenatal phenotypic overlap of Costello syndrome and severe Noonan syndrome by tridimensional ultrasonography. Prenat Diagn 26:340–344.

Lo IF, Brewer C, Shannon N, Shorto J, Tang B, Black G, Soo MT, Ng D, Lam ST, Kerr B. 2008. Severe neonatal manifestations of Costello syndrome. J Med Genet 45:167–171.

Nava C, Hanna N, Michot C, Pereira S, Pouvreau N, Niihori T, Aoki Y, Matsubara Y, Arveiler B, Lacombe D, Pasmant E, Parfait B, Baumann C, Héron D, Sigaudy S, Toutain A, Rio M, Goldenberg A, Leheup B, Verloes A, Cavé H. 2007. Cardio-facio-cutaneous and Noonan syndromes due to mutations in the RAS/MAPK signalling pathway: Genotype-phenotype relationships and overlap with Costello syndrome. J Med Genet 44:763–771.

Rauen KA. 2007. HRAS and the Costello syndrome. Clin Genet 71: 101–108.

Schulz AL, Albrecht B, Arici C, van der Burgt I, Buske A, Gillessen-Kaesbach G, Heller R, Horn D, Hübner CA, Korenke GC, König R, Kress W, Krüger G, Meinecke P, Mücke J, Plecko B, Rossier E, Schinzel A, Schulze A, Seemanova E, Seidel H, Spranger S, Tuysuz B, Uhrig S, Wieczorek D, Kutsche K, Zenker M. 2008. Mutation and phenotypic spectrum in patients with cardio-facio-cutaneous and Costello syndrome. Clin Genet 73:62–70.

Sol-Church K, Stabley DL, Nicholson L, Gonzalez IL, Gripp KW. 2006. Paternal bias in parental origin of HRAS mutations in Costello syndrome. Hum Mutat 27:736–741.

Van den Bosch T, Van Schoubroeck D, Fryns JP, Naulaers G, Inion AM, Devriendt K. 2002. Prenatal findings in a monozygotic twin pregnancy with Costello syndrome. Prenat Diagn 22:415–417.

Zampino G, Pantaleoni F, Carta C, Cobellis G, Vasta I, Neri C, Pogna EA, De Feo E, Delogu A, Sarkozy A, Atzeri F, Selicorni A, Rauen KA, Cytrynbaum CS, Weksberg R, Dallapiccola B, Ballabio A, Gelb BD, Neri G, Tartaglia M. 2007. Diversity, parental germline origin, and phenotypic spectrum of de novo HRAS missense changes in Costello syndrome. Hum Mutat 28:265–272.

RESEARCH ARTICLE

AMERICAN JOURNAL OF medical genetics PART A

A Locus for Ophthalmo-Acromelic Syndrome Mapped to 10p11.23

Haruka Hamanoue,[1,2] Andre Megarbane,[3] Takaya Tohma,[4] Akira Nishimura,[1] Takeshi Mizuguchi,[1] Hirotomo Saitsu,[1] Haruya Sakai,[1] Shoko Miura,[5] Tatsushi Toda,[6] Noriko Miyake,[1] Norio Niikawa,[5] Koichiro Yoshiura,[5] Fumiki Hirahara,[2] and Naomichi Matsumoto[1]*

[1]Department of Human Genetics, Yokohama City University Graduate School of Medicine, Yokohama, Japan

[2]Department of Obstetrics and Gynecology, Yokohama City University Graduate School of Medicine, Yokohama, Japan

[3]Medical Genetics Unit, St. Joseph University, Beirut, Lebanon

[4]Division of Pediatrics, Okinawa Prefectural Nanbu Medical Center & Children's Medical Center, Haebaru, Japan

[5]Department of Human Genetics, Nagasaki University Graduate School of Biomedical Sciences, Nagasaki, Japan

[6]Division of Clinical Genetics, Department of Medical Genetics, Osaka University Graduate School of Medicine, Suita, Japan

Received 29 July 2008; Accepted 10 October 2008

Ophthalmo-acromelic syndrome (OAS, OMIM %206920) is a rare autosomal recessive disease, presenting with clinical anophthalmia and limb anomalies. We recruited three OAS families including a Japanese family with two affected patients and two consanguineous Lebanese families each having an affected. Homozygosity mapping was performed using the 50K SNP chip and additional informative markers. A locus for OAS was mapped to the 422-kb region at 10q11.23, based on the results from the two consanguineous families as well as the consistent data from the Japanese non-consanguineous family. The 422-kb region only contained one gene, *MPP7*. Although we could not detect any pathological mutations in OAS families analyzed, *MPP7* could remain a candidate as aberrant changes might exist beyond our mutation detection methods. Further families are needed to confirm this candidate locus. © 2009 Wiley-Liss, Inc.

Key words: ophthalmo-acromelic syndrome; linkage study; genetic locus; 10p11.23

How to Cite this Article:
Hamanoue H, Megarbane A, Tohma T, Nishimura A, Mizuguchi T, Saitsu H, Sakai H, Miura S, Toda T, Miyake N, Niikawa N, Yoshiura K, Hirahara F, Matsumoto N. 2009. A locus for ophthalmo-acromelic syndrome mapped to 10p11.23.
Am J Med Genet Part A 149A:336–342.

INTRODUCTION

Ophthalmo-acromelic syndrome (OAS, OMIM %206920), also known as Waardenburg's recessive anophthalmia syndrome, is a rare autosomal recessive disorder, presenting with anophthalmia or microphthalmia and limb anomalies. Since the first report by Waardenburg [1961], at least 35 cases from 21 families have been reported [Richieri-Costa et al., 1983; Pallotta and Dallapiccola, 1984; Traboulsi et al., 1984; Le Merrer et al., 1988; al Gazali et al., 1994; Quarrell, 1995; Sayli et al., 1995; Suyugul et al., 1996; Megarbane et al., 1998; Cogulu et al., 2000; Tekin et al., 2000; Caksen et al., 2002; Kara et al., 2002; Garavelli et al., 2006; Teiber et al., 2007]. Majority of OAS families are consanguineous (~90%) [Garavelli et al., 2006]. Ocular phenotypes in OAS widely range from mild microphthalmia to true anophthalmia [Kara et al., 2002]. Typical limb malformations include fused 4th and 5th metacarpals and short 5th finger in hands and olygodactyly in foot (four toes) [Teiber et al., 2007]. Most cases have bilateral anophthalmia/microphthalmia (88%), but unilateral abnormality is also noted. Other (visceral) malformations are rare, but venous or vertebral anomaly was recognized each in single cases [Tekin et al., 2000; Teiber et al., 2007].

The genetic cause for OAS remains undetermined. Genome-wide homozygosity mapping was undertaken and a locus for OAS was identified using three families including four affected individuals. A possible responsible gene will be discussed.

Grant sponsor: Ministry of Health, Labour and Welfare; Grant sponsor: SORST; Grant sponsor: Scientific Research from the Ministry of Education, Sports, Science and Technology, Japan.

*Correspondence to:
Naomichi Matsumoto, M.D., Ph.D, Department of Human Genetics, Yokohama City University Graduate School of Medicine, Fukuura 3-9, Kanazawa-ku, Yokohama 236-0004, Japan.
E-mail: naomat@yokohama-cu.ac.jp

Published online 10 February 2009 in Wiley InterScience (www.interscience.wiley.com)
DOI 10.1002/ajmg.a.32656

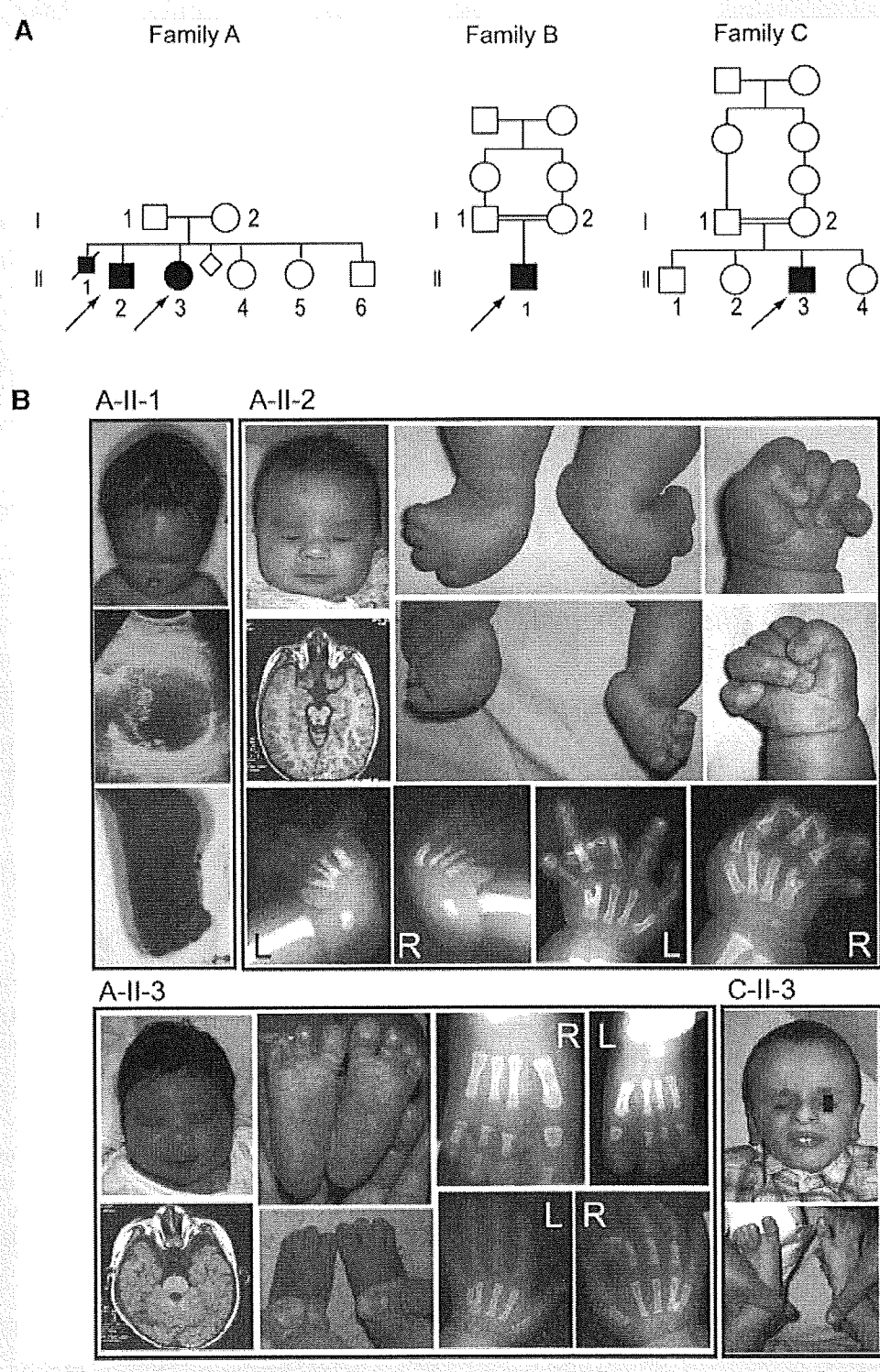

FIG. 1. Three OAS families used for this study and clinical manifestations of families A and C. A: Three OAS-family pedigrees are shown. Family A (Japanese) has two affected individuals and one affected abortus, family B (Lebanese) one affected born from the consanguineous parents, and family C (Lebanese) one affected also from the consanguineous parents. B: Clinical features of one affected abortus (A-II-1) and two affected individuals (A-II-2 and A-II-3) in family A and an affected individual (C-II-3) in family C. A-II-1 showed bilateral microphthalmia, adherent eyelids, bilateral oligodactyly (absence of 1st toes), cleft lip/palate and holoprosencephaly with hydrocephaly. A-II-2 at age of 6 years and A-II-3 at 5 years both presented with bilateral anophthalmia (confirmed by brain MRI), closed eyelids and limb anomalies with bilateral metacarpal synostosis between the 4th and 5th fingers and bilateral oligodactyly (absence of 1st toes). C-II-3 at age of 2 years showed bilateral anophthalmia and distal limb abnormalities including bilateral syndactyly of 2nd to 5th toes with symphysis.

MATERIALS AND METHODS

Patients and Their Families

Three families with one or two cases of OAS were analyzed in this study (Fig. 1 and Table I). In family A, two affected sibs (A-II-2 at 6 years and A-II-3 at 5 years) both presented with bilateral anophthalmia, closed eyelids and limb anomalies with bilateral metacarpal synostosis between the 4th and 5th fingers and bilateral oligodactyly (absence of 1st toes). In this family, their first child was a stillborn son (A-II-1), who had bilateral microphthalmia, adherent eyelids, bilateral oligodactyly (absence of 1st toes), cleft lip/palate and holoprosencephaly with hydrocephaly. Though no evidence of consanguinity was obtained, their eight grandparents were all originated from the Okinawa island in Japan. The other two families (B and C) were independent consanguineous Lebanese families, of which the family B was previously reported [Megarbane et al., 1998]. The proband B-II-1, a 10-year-old boy, was the first child of healthy parents, presenting with bilateral anophthalmia, adherent eyelids, deeply set orbits, anteverted nares, normally positioned ears, a normal philtrum, thin lips, micrognathia, very short neck, narrow chest, bilateral upper limb anomalies (split hands: four digits on the right hand and two digits on the left), and six short toes on the right foot (right postaxial polydactyly) [Megarbane et al., 1998]. These limb abnormalities are atypical for OAS. The patient, C-II-3, a 2-year-old boy, showed bilateral anophthalmia and distal limb abnormalities including bilateral syndactyly of 2nd to 5th toes. A total of 4 affected and 12 unaffected members from the three families were analyzed. Genomic DNA was obtained from peripheral blood leukocytes using QuickGene 610-L (FUJIFILM, Tokyo, Japan) after informed consent. Experimental protocols were approved by the Institutional Review Board at Yokohama City University School of Medicine.

SNP Genotyping

Whole SNP genotyping was undertaken using the GeneChip™ Human Mapping 50K Array *Xbal* (Affymetrix, Inc., Santa Clara, CA) containing 58,625 SNPs (single nucleotide polymorphism) according to the manufacture's protocols. In brief, 250 ng DNA was digested with *Xba*l. The adaptors were ligated to the digested DNA, and the ligation-mediated PCR with single-primer was performed. PCR products were purified by microcon YM-100 (Millipore, Inc., Billerica, MA). The product was fragmented, end-labeled, and hybridized to an array. SNP markers on the chip are almost equally distributed in the whole genome, with mean marker-distances of

TABLE I. Clinical Features of OAS Patients

	A-II-1	A-II-2	A-II-3	B-II-1	C-II-3
Origin	Okinawa, Japan	Okinawa, Japan	Okinawa, Japan	Lebanon	Lebanon
Consanguinity	−	−	−	+	+
Sex	Male	Male	Female	Male	Male
Eye abnormality	+	+	+	+	+
Anophthalmia	Bilateral	Bilateral	Bilateral	Bilateral	Bilateral
Loss of optic nerve (CT)	n.c.	Bilateral	Bilateral	Bilateral	Bilateral
Loss of optic tract (CT)	n.c.	+	+	−	−
Upper limb abnormality	+	+	+	+	+
Oligodactyly	n.c.	−	−	Right oligodactyly/ left lobster-claw	−
Metacarpal synostosis	n.c.	4th and 5th fingers	4th and 5th fingers	2nd and 3rd fingers	−
Clinodactyly	+	+	−	+	+
Camptodactyly	n.c.	+	−	+	+
Single transverse palmar crease	n.c.	+	+	n.c.	−
Lower limb abnormality	+	+	+	+	+
Oligodactyly/polydactyly/syndactyly	Bilateral oligodactyly	Bilateral oligodactyly	Bilateral oligodactyly	Right polydactyly	Bilateral syndactyly
Metatarsal synostosis	n.c.	+	+	+	−
Tibia valga	n.c.	+	+ (mild)	n.c.	−
Hypoplastic fibula	n.c.	+	+ (mild)	n.c.	−
Abnormal cleavage between toes	n.c.	1st and 2nd toes	1st and 2nd toes	−	1st and 2nd toes
Dermal syndactyly	n.c.	2nd and 3rd toes	2nd and 3rd toes	−	2nd to 5th toes
Talipes valgus	−	+	−	+	−
Other					
Holoprosencephaly	+	−	−	−	−
Cleft palate	+	−	−	−	−
Failure to thrive	n.c.	+	+	+	+
Developmental retardation	n.c.	DQ = 10	DQ = 15	+	+
Cryptorchidism	n.c.	Right		−	n.c.

n.c., not confirmed.

23.6 kb and an average heterozygosity of 0.30 among African American, European, and Asian. SNP calling, signal intensity data, and Mendelian error in each pedigrees to exclude conflicted SNPs were checked using GCOS 1.2 (the GeneChip Operating Software) platform (Affymetrix) and the Batch analysis in GTYPE 4.0 (GeneChip Genotyping Analysis Software) (Affymetrix), with the default setting for mapping algorithm. CNAG (Copy Number Analyser for GeneChip) Ver. 2.0 was also used to validate copy number alterations as well as loss of heterozygosity (LOH).

Linkage Analysis

Multipoint linkage analysis using aligned SNPs was performed using ALLEGRO software [Gudbjartsson et al., 2000, 2005]. Two-point linkage analysis of candidate regions was also performed using the LINKAGE package, MLINK (FASTLINK software, ver. 5.1). In each program, autosomal recessive model of inheritance with complete penetrance and a disease allele frequency of 0.001 were applied.

Fine Mapping With Short Tandem Repeat Markers

Fine mapping of possible candidate regions using additional microsatellite markers was done as previously described [Kondo et al., 2004]. Most markers were designed according to the Marshfield genetic map (http://research.marshfieldclinic.org/genetics). If appropriate markers were not found, candidate di-, tri-, and tetranucleotide repeat markers were originally selected from regions of interest using the UCSC genome browser (March 2006 assembly), and PCR primers were designed with the Primer3 program.

TABLE II. Primer Information of Markers

Marker	Forward (5′ > 3′)	Reverse (5′ > 3′)	Fluorescence	Product size (bp)	Annealing temperature (°C)
D10S1653[a]	CCTTTGGATAAAGCCTCCT	TATCATTGTCTCATCCGGG	VIC	201–213	55
D10S1661[a]	ACGCTACTTGCCAGGTC	ATTGCTTCCCTGAGAGTGT	VIC	250–272	58
D10S1476[a]	TGACTAAACAGACCCAGACTTG	GAACGCATGTCCACCCTA	NED	250–266	62
D10S504[a]	TCAGGTATTTCTTCATAGCAG	TTCCCTTGCTCTGCAGCTT	NED	366–370	62
D10S1125[a]	TGGTGGCCTCTTACCTAG	CCATTTGTATGTGTTCTCTTGAG	NED	225–249	64
D10S466[a]	CTGGGCCACAGTGAGACT	TAGGTCATCTGGTCTTCCATAC	NED	120–140	60
D10S1734[a]	GCCTGGGTGACAGAGTGAGATTCTA	ACACACGTACACATGGGGTGGT	NED	163–189	64
D10S1789[a]	TTTCCCACTCCAGTGC	TCATAGATAGAGACCATTAGTTTCA	VIC	134–150	60
D10S1673[a]	CCAACCTGGATGACAGAGC	CTTACCCCCAACCAAAGGAC	VIC	198–216	64
D10S1747[a]	TGTAGACCAGTAGACCATGACAAAT	CCACAGTCAGATATAGTGTGCAA	FAM	117–123	64
STS1[c]	TGTCCATCTCTTCAAACACTGG	TCCTGGGAATAGCGTTCACT	NED	243	60
AFM290XE1[a]	ATTTTTGACATTGTCCCA	CTAAGCCCTAGCACCTTT	FAM	247	57
AFM295TH1[a]	TATTATACTCCAGCCGGGG	GGAGACTATTTACTTTGTGTCCTTG	FAM	130	63
STS2[c]	TGGATATGAAAAGGGGTGATAA	GGTCCAGATGGTACTCACACG	FAM	246	60
STS3[c]	TGGGCTGCACATTTATACCA	TGTGACCTGCTCCTCACAAG	FAM	169	60
STS4[c]	TGATGTGTGTGTATTTTGTGTGTG	ACTCTTTGCAGCATCCCAGT	FAM	226	60
STS5[c]	TCTGTGTGCAGCTCCTCAGT	ACCTGGACAGGATCATCTGG	NED	224	60
D10S572[a]	CAGTGATTTTAGACAGGGATTTTA	AATTATGATACTTATTGATGGGGA	NED	275–283	63
D10S2481[b]	TGGAAGTTATGGACCAGGAA	CCAATGTCCAGCTAAGTGAGG	VIC	312	60
D10S197[a]	ACCACTGCACTTCAGGTGAC	GTGATACTGTCCTCAGGTCTCC	FAM	161–173	55
STS6[c]	TGCATTTAAGGAGAATCAGTTG	GCAGTGACTGTTCAAGATTTTTGT	FAM	194	60
STS7[c]	TGAACTACTGCTCTCAAATCTGTGT	GGGACACAATGGCTTTGAAC	VIC	157	60
STS8[c]	TTGGATTTTATTTGAAAATTAGGG	TTGGTTGGCTGAATAACTTCC	FAM	213	60
STS9[c]	GCTAATCCAGAGATACCACCAGA	CCTAGTTTGCTGAGACTGTTGTG	NED	371	60
STS10[c]	CCCTAGAAGTATTTGAAGAAGTAGCA	TGTGGTGCTCTTTCCTGTGA	NED	108	60
STS11[c]	GCTCAGTGGGACAATTCATGT	GAATAATGCCCCCGAAAGAT	VIC	399	60
STS12[c]	GCTGTTGGCTGTGAGTTCAA	CCCTTGGGCTTGGACTAGAA	FAM	388	60
UT541[a]	ATGGGGGTAGAGGGTCTGG	CAGCCTGGGTGACAAAGTCT	NED	143–340	60
AFMB345YA9[a]	GGAACCTAAGGCATGTTGAT	CCAAGACCCTGTCTGAAAAA	FAM	151–171	60
GATA29G05[a]	TGCTTATATCCAGCTAATATAAATG	CCATGAGGTTTATTTTCCCC	FAM	108–172	60
AFM095ZH7[a]	TATATGCAGTTTGGGATGGG	ATTGGGCTGTGCCTACACTT	VIC	213–231	60
D10S208[a]	AGGTGACTGTTTTGGGGGAG	GAGTGTGGGGATGTTTTCAA	NED	170–186	55
AFM137XH4[a]	AACATCCATTTGGAGAATTAAAAT	TACAGTGTGATTGCACGACT	NED	171–183	60
AFM353TB5[a]	TCAGTGGGAACGTAAATCAG	AGCTGAATATTATTCCATTGTGAGT	NED	175	58
D10S196[a]	TTCAAAGGTGGAGACCCTTC	TTTTGGTCAGAATGGAGTGG	VIC	99–109	55

[a]Primers for known microsatellite marker.
[b]Primers for known microsatellite marker with our modification.
[c]Newly designed primers.

Fluorescent-labeled (either FAM, VIC, or NED) forward primers and tailed reverse primers were purchased from Applied Biosystems (Tokyo, Japan). PCR products for each marker were electrophoresed on ABI Prism Genetic Analyzer 3100 (Applied Biosystems), and analyzed using GeneMapper Software ver. 3.5 (Applied Biosystems). PCR was cycled 40 times at 94°C for 30 sec, at 55–64°C for 30 sec and at 72°C for 30 sec in a total volume of 10 μl, containing 30 ng of genomic DNA as a template, 0.5 μM of each primer, 200 μM of each dNTP, 1× ExTaq buffer and 0.25 U ExTaq (Takara Bio, Inc., Ohtsu, Japan). Haplotype blocks were constructed manually. The list of primers is presented in Table II.

Mutation Analysis of a Candidate Gene

All coding exons and exon-intron boundaries together with 5′- and 3′-untranslated regions of *MPP7* (Membrane protein, palmitoylated 7) were analyzed. PCR was cycled 35 times at 94°C for 30 sec, at 60°C for 30 sec and at 72°C for 30–90 sec in a total volume of 20 μl containing 30 ng of genomic DNA as a template, 0.5 μM of forward and reverse primers, 200 μM of each dNTP, 1× ExTaq buffer, and 0.25 U of ExTaq (Takara Bio, Inc.). All primers were designed using the Primer3 software. Detailed information of *MPP7* primers is available on request. PCR products were purified with ExoSAP™ (USB Co., Cleveland, OH) and sequenced using BigDye Terminator 3.1 (Applied Biosystems) on the 3100 Genetic Analyzer. Sequences of patients were compared to the reference genome sequences in the UCSC Genome Browser (Mar 2006 assembly) using the Seqscape software ver. 2.1 (Applied Biosystems).

Expression Study of Mpp7 in Mouse Tissues

Whole head tissues from mice embryos at E10.5, eyeball, forelimb and hindlimb tissues from embryos each at E12.5, 13.5, and 16.5 were collected. Total RNA was extracted from collected tissues using Trizol reagent (Invitrogen, Carlsbad, CA). Two micrograms of RNA was reverse-transcribed in a volume of 20 μl using PrimeScript 1st strand cDNA Synthesis kit (Takara Bio, Inc). RT-PCR analysis was started at 94°C for 5 min as a first denaturing step, then cycled 25, 30, or 35 times at 94°C for 30 sec, at 56°C for 30 sec and at 72°C for 30 sec in a volume of 25 μl, containing 2 μl of reverse transcription reaction as a template, 0.2 μM of each primer, 400 μM of each dNTP, 1× ExTaq buffer and 0.125 U ExTaqHS (Takara Bio, Inc). Primers for RT-PCR were as follows: *Mpp7*-1-F, 5′-TGTATGAGCTGTTGGCTGCT-3′, and *Mpp7*-1-R, 5′-AGCCTT-

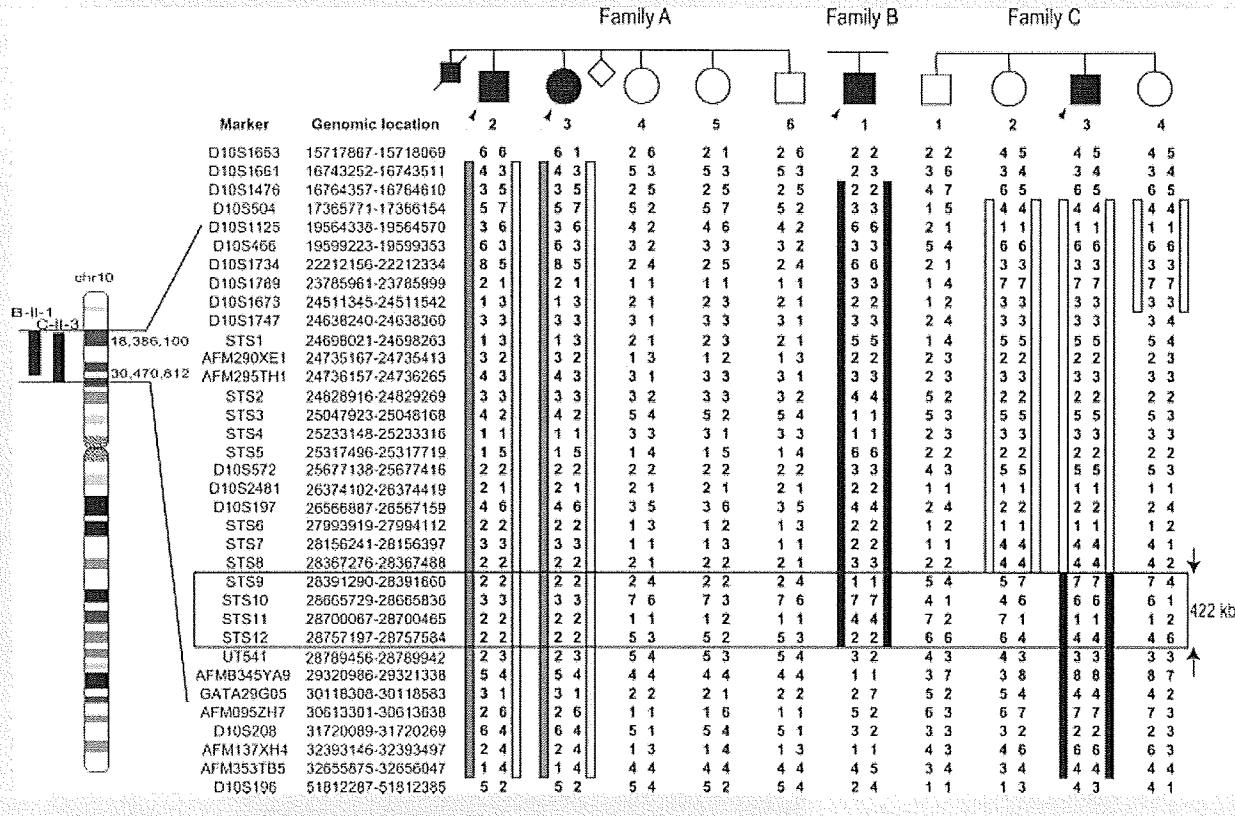

FIG. 2. Homozygosity mapping and haplotypes of three OAS families. Pedigrees of the three OAS families (Top). Chromosome 10 ideogram and IBD regions of B-II-1 and C-II-3 revealed by Affymetrix GeneChip 50K array are indicated with black bars. Polymorphic markers around IBD regions and haplotypes are indicated in all families. In families B and C, the common IBD region was mapped to a 422-Kb region, flanked by marker *STS8* and *UT541*. Affected sibs in Family A (II-2 and II-3) possess heterozygous haplotype blocks (shown as gray bars), probably implying compound heterozygous mutations.

GACATTGGGTTTTG-3′; *Mpp7*-2-F, 5′-AGCCTTGACATTGGG-TTTTG-3′, and *Mpp7*-2-R, 5′-TTATGAATGTAACCAACTCAC-TGG-3′. To ensure equal loading of cDNA into RT-PCR reactions, *B2m* cDNA was amplified as an internal control using the following primers: *B2m*-F, 5′-TGGTGCTTGTCTCACTGACC-3′, and *B2m*-R, 5′-TGCTTAACTCTGCAGGCGTAT-3′.

RESULTS AND DISCUSSION

Linkage analysis using ALLEGRO program revealed 16 candidate loci showing the LOD score ($\theta = 0.000$) higher than 3.0 (data not shown). All candidate regions except for a region of chromosome 10 (SNP blocks from rs7920803 to rs7094225 with the maximum LOD score, 3.9880) were ruled out by additional microsatellite markers as they did not show a pattern of identical by descent (IBD). LOH analysis using the CNAG program confirmed that B-II-1 and C-II-3 shared only one consistent region at chromosome 10. The region was comprised of 303 consecutive SNPs from rs1986480 to rs10508745, spanning approximately an 11-Mb segment at 10p12.33–p11.23 (Fig. 2). In contrast, A-II-2 and A-II-3 did not show any blocks of IBD, suggesting that it is unlikely that that their parents had a common ancestor. Further fine mapping using more markers confirmed that an affected individual (C-II-3) and an unaffected individual (C-II-2) shared the same homozygous genotype's region from *D10S504* to *STS8*. Thus the candidate region was narrowed down to a 422-kb segment from *STS9* and *STS12* at 10p11.23 through the analysis of families B and C. ALLEGRO program using all families indicated the maximum multi-point LOD score was 3.9863 near *STS9*. MLINK showed a maximum two-point LOD score was 2.9444 ($\theta = 0.000$) at *STS10*. Within the 422-kb region, only one established gene, *MPP7* (palmitoylated membrane protein 7) was located. Mutation screening of *MPP7* could not detect any abnormalities. All the haplotypes of the 422-kb segment in the three families are different.

Homozygosity mapping of two consanguineous Lebanese families each having an affected child revealed a candidate locus from *STS9* to *STS12*, a 422-kb region under the hypothesis that OAS is an autosomal recessive disorder. Though we initially expected that broad and many chromosomal regions might be highlighted as IBD, only a narrow 10p11.23 segment turned out to be a region of interest. Two affected sibs (A-II-1 and A-II-2) were likely to have less and smaller IBD regions as the family was not consanguineous. Indeed, we could not confirm any IBD regions on the Affymetrix 50K SNPs, suggesting that the two patients in the family A have compound heterozygous mutations.

Although *MPP7* is the only gene mapped to the 440-kb region and *Mpp7* is expressed in head tissues at E10.5, and in eyeballs and limbs at E12.5–E16.5 (Fig. 3), no causative mutations were found in our patients. This could be due to the limit of analytical methods. For example, mutations of promoter regions or small intragenic deletions/duplications might not be detected, though the Affymetrix GeneChip 50K could not detect any copy number changes of the region. Further investigation is absolutely necessary.

OAS is a very rare syndrome, usually the eye sign is consistent but the limb abnormalities are variable, so it is possible that OAS may have locus heterogeneity with different subtypes. As families B and

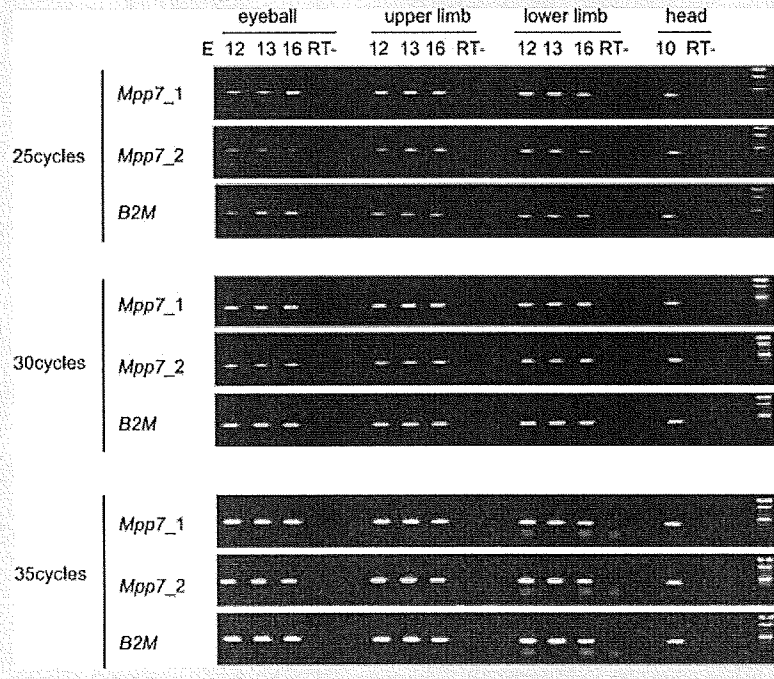

FIG. 3. Mpp7 expression analysis in mice embryonic tissues. *Mpp7* expression is confirmed using two different primer sets in all tissues examined by 25-, 30-, 35-cycled RT-PCR. Eyeball, upper and lower limb tissues at E12.5, E13.5, and E16.5, and whole head tissues at E10.5 were examined. *B2M* is an internal control gene.

C are of the same ethnic origin and were clinically examined by one of coauthors (M.A), we expected the similar haplotype for the two families. However, haplotypes of the 422-kb homozygous region are different between the two families. Thus the two families may not be caused by the same ancestral mutation. More families, if available, should be investigated.

In conclusion, a locus for OAS is validated by SNP homozygosity mapping. It is a 422-kb segment at 10p11.23 corresponding to *MPP7*, but no mutation was found. The SNP homozygosity mapping is very useful for autosomal recessive traits even if only a few families are available for study, but of course, more patients and families are definitely useful for this type of analysis.

ACKNOWLEDGMENTS

Patients and their families, all the collaborating doctors are highly appreciated. Research Grants from the Ministry of Health, Labour and Welfare (N.M.); SORST from JST (N.M. and N.N.); and Grant-in-Aid for Scientific Research from the Ministry of Education, Sports, Science and Technology, Japan (N.M.)

REFERENCES

al Gazali LI, Sabarinathan DK, Khidir A. 1994. Microphthalmia and distal limb abnormalities in a child of consanguineous parents. Clin Dysmorphol 3:258–262.

Caksen H, Odabas D, Oner AF, Abuhandan M, Calebi V. 2002. Ophthalmo-acromelic syndrome in a Turkish infant: Case report. East Afr Med J 79:339–340.

Cogulu O, Ozkinay F, Gunduz C, Sapmaz G, Ozkinay C. 2000. Waardenburg anophthalmia syndrome: Report and review. Am J Med Genet 90:173–174.

Garavelli L, Pedori S, Dal Zotto R, Franchi F, Marinelli M, Croci GF, Bellato S, Ammenti A, Virdis R, Banchini G, Superti-Furga A. 2006. Anophthalmos with limb anomalies (Waardenburg opththalmo-acromelic syndrome): Report of a new Italian case with renal anomaly and review. Genet Couns 17:449–455.

Gudbjartsson DF, Jonasson K, Frigge ML, Kong A. 2000. Allegro, a new computer program for multipoint linkage analysis. Nat Genet 25:12–13.

Gudbjartsson DF, Thorvaldsson T, Kong A, Gunnarsson G, Ingolfsdottir A. 2005. Allegro version 2. Nat Genet 37:1015–1016.

Kara F, Yesildaglar N, Tuncer RA, Semerci N, Onat N, Yilmazer YC, Sipahi T, Erkaya S. 2002. A case report of prenatally diagnosed ophthalmo-acromelic syndrome type Waardenburg. Prenat Diagn 22:395–397.

Kondo H, Qin M, Mizota A, Kondo M, Hayashi H, Hayashi K, Oshima K, Tahira T, Hayashi K. 2004. A homozygosity-based search for mutations in patients with autosomal recessive retinitis pigmentosa, using microsatellite markers. Invest Ophthalmol Vis Sci 45:4433–4439.

Le Merrer M, Nessmann C, Briard ML, Maroteaux P. 1988. Ophthalmo-acromelic syndrome. Ann Genet 31:226–229.

Megarbane A, Souraty N, Tamraz J. 1998. Ophthalmo-acromelic syndrome (Waardenburg) with split hand and polydactyly. Genet Couns 9:195–199.

Pallotta R, Dallapiccola B. 1984. A syndrome with true anophthalmia, hand-foot defects and mental retardation. Ophthalmic Paediatr Genet 4:19–23.

Quarrell OW. 1995. Ophthalmo acromelic syndrome. Clin Dysmorphol 4:272–273.

Richieri-Costa A, Gollop TR, Otto PG. 1983. Brief clinical report: Autosomal recessive anophthalmia with multiple congenital abnormalities–type Waardenburg. Am J Med Genet 14:607–615.

Sayli BS, Akarsu AN, Altan S. 1995. Anophthalmos-syndactyly (Waardenburg) syndrome without oligodactyly of toes. Am J Med Genet 58:18–20.

Suyugul Z, Seven M, Hacihanefioglu S, Kartal A, Suyugul N, Cenani A. 1996. Anophthalmia-Waardenburg syndrome: A report of three cases. Am J Med Genet 62:391–397.

Teiber ML, Garrido JA, Barreiro CZ. 2007. Ophthalmo-acromelic syndrome: Report of a case with vertebral anomalies. Am J Med Genet Part A 143A:2460–2462.

Tekin M, Tutar E, Arsan S, Atay G, Bodurtha J. 2000. Ophthalmo-acromelic syndrome: Report and review. Am J Med Genet 90:150–154.

Traboulsi EI, Nasr AM, Fahd SD, Jabbour NM, Der Kaloustian VM. 1984. Waardenburg's recessive anophthalmia syndrome. Ophthalmic Paediatr Genet 4:13–18.

Waardenburg PJ. 1961. Autosomally-recessive anophthalmia with malformations of the hand and feet. Genet Ophthalmol 772.

Searching for Genes for Cleft Lip and/or Palate Based on Breakpoint Analysis of a Balanced Translocation t(9;17)(q32;q12)

Junichiro Machida, D.D.S., Ph.D., Têmis M. Félix, M.D., Ph.D., Jeffrey C. Murray, M.D., Koh-ichiro Yoshiura, M.D., Ph.D., Mitsuyo Tanemura, M.D., Ph.D., Munefumi Kamamoto, D.D.S., Kazuo Shimozato, D.D.S., Ph.D., Shin-ichi Sonta, Ph.D., Takao Ono, Ph.D.

Objective: **Identification of the breakpoints of disease-associated chromosome rearrangements can provide informative clues to a positional cloning approach for genes responsible for inherited diseases. Recently, we found a three-generation Japanese family segregating balanced chromosome translocation t(9;17)(q32;q12). One of the subjects had cleft lip and palate. We examined whether regions near the breakpoint could be associated with cleft lip and/or palate.**

Methods: **We determined the breakpoints involved in the translocation by fluorescence *in situ* hybridization analysis and subsequent long-range polymerase chain reaction. In order to study the role of these disrupted regions in nonsyndromic cleft lip and/or palate, we performed mutation analysis and a haplotype-based transmission disequilibrium test using tagging single-nucleotide polymorphisms in the flanking regions of the breakpoints in white and Filipino nonsyndromic cleft lip and/or palate populations.**

Results: **Sequence analysis demonstrated that two genes, *SLC31A1* (solute carrier family 31 member 1) on chromosome 9 and *CCL2* (chemokine ligand 2) on chromosome 17, were rearranged with the breaks occurring within their introns. It is interesting that *SLC31A1* lies closed to *BSPRY* (B-box and SPRY domain), which is a candidate for involvement with cleft lip and/or palate. Some of the variants in *BSPRY* and *CCL2* showed significant *p* values in the cleft lip and/or palate population compared with the control population. There was also statistically significant evidence of transmission distortion for haplotypes on both chromosomes 9 and 17.**

Conclusions: **The data support previous reports that genes on chromosomal regions of 9q and 17q play an important role in facial development.**

KEY WORDS: *association analysis, balanced chromosomal translocation,* BSPRY, CCL2, *cleft lip and palate, haplotype, HapMap,* SLC31A1

Nonsyndromic cleft lip and/or palate (CL/P) is a common congenital anomaly of complex etiology, with the birth prevalence being approximately 1 per 700 live births (Mossey and Little, 2002; Murray, 2002). Previous family and population studies indicate that both genetic and environmental factors are involved in the occurrence of this malformation. Prior sequencing analysis of CL/P has indicated roles for mutations in *MSX1*, *FOXE1*, *GLI2*, *MSX2*, *SKI*, *SPRY2*, *RYK*, *FGF1*, *FGF2*, and *FGF8* in the etiology of the birth defect (Ichikawa et al., 2006; Jezewski et al., 2003; Riley et al., 2007; Vieira et al., 2005). In addition, polymorphisms in *IRF6* have been found to be associated with CL/P (Blanton et al., 2005; Ghassibe et al., 2005; Park et al., 2007; Scapoli et al., 2005; Zucchero et al., 2004).

Dr. Machida is Associate Professor, Department of Maxillofacial Surgery, School of Dentistry, Aichi-Gakuin University, Nagoya, Japan. Dr. Félix is Clinical Geneticist, Medical Genetics Service of Hospital de Clínicas de Porto Alegre, Porto Alegre, Brazil. Dr. Murray is Professor, Department of Pediatrics, University of Iowa, Iowa City, Iowa. Dr. Yoshiura is Professor, Department of Human Genetics, Graduate School of Biomedical Sciences, Nagasaki University, Nagasaki, Japan. Dr. Tanemura is Associate Professor, Department of Obstetrics and Gynecology, Nagoya City University Graduate School of Medical Sciences, Nagoya, Japan. Dr. Kamamoto is postgraduate student and Dr. Shimozato is Professor, Department of Maxillofacial Surgery, School of Dentistry, Aichi-Gakuin University, Nagoya, Japan. Dr. Sonta is Chief Scientist, Division of Cytogenetics, Department of Genetics, Institute for Developmental Research, Aichi Human Service Center, Kasugai, Japan. Dr. Ono is Senior Research Scientist, Chromosome Dynamics Laboratory, RIKEN Discovery Research Institute, Wako, Saitama, and Senior Researcher, Division of Clinical Genetics, Department of Genetics, Institute for Developmental Research, Aichi Human Service Center, Kasugai, Japan.

Funding was provided by the Grant-in-Aid for Young Scientists of Japan Society for the Promotion of Science 16791271 and National Institutes of Health grants DE08559 (J.C.M.) and DE016215 (J.C.M.).

Submitted August 2008; Accepted January 2009.

Address correspondence to: Dr. Junichiro Machida, Department of Maxillofacial Surgery, School of Dentistry, Aichi-Gakuin University, 2-11 Suemori-dori, Chikusa-ku, Nagoya 464-8651, Japan. E-mail jmachida@dpc.aichi-gakuin.ac.jp.

DOI: 10.1597/08-047.1

Because clefts are complex and caused by multiple interacting genes, we do not expect that single gene disruptions in all individuals with a chromosomal break will manifest as CL/P. However, in some cases, identification of the breakpoints of disease-associated chromosome translocations can be an effective way to identify genes and/or chromosomal regions contributing to the occurrence of CL/P. The positional cloning approach for disease-associated genes using chromosome rearrangements has successfully identified four relevant genes (*CLPTM1* [Yoshiura et al., 1998], *SATB2* [FitzPatrick et al., 2003], *SUMO1* [Alkuraya et al., 2006], and *FGFR1* [Kim et al., 2005]) as candidates for CL/P. These findings suggest that identification of the genes disrupted in a cleft/translocation case can give us insight into some of the pathways involved in this birth defect and provide candidates for analysis in cases independent of the index family.

Recently, we identified a Japanese family segregating a balanced chromosome translocation t(9;17)(q32;q12). Of three generations we examined, one individual is affected with cleft lip and palate. Genome-wide linkage studies have suggested that the region 9q21 has significant linkage with CL/P (Marazita et al., 2004). Therefore, genes in this region of chromosome 9 may have an important role in facial development. In this study, we identified the breakpoints of t(9;17)(q32;q12) in the patient by fluorescence *in situ* hybridization (FISH) analysis and identified candidate genes by polymerase chain reaction (PCR) and DNA sequencing. We then carried out a mutation search and a case-control association study of candidate genes. In addition, extended single-nucleotide polymorphism (SNP) analysis of the chromosomal regions adjacent to the translocation breakpoint was performed.

Materials and Methods

Clinical Report

The proband was a male infant born prematurely by cesarean section at 24 weeks gestation after an uneventful pregnancy. The maternal age was 25 years and paternal age 26 years at the time of his birth. The parents were nonconsanguineous, and there was no family history of malformations. His birth weight and height were 706 g and 31.8 cm, respectively (10th centile = 560 g, 90th centile = 774 g). The patient was in normal development at 24 weeks gestation. The circumferences of his head and chest were 23 cm and 21 cm at birth, respectively. He had apparent ocular hypertelorism, a bilateral cleft lip and palate, and a mild nasal flattening. Echocardiography showed a small atrial septal defect, which had closed by 2 years of age. At 6 years after birth, his weight and height were normal for age at 20.1 kg and 114.6 cm, respectively. He shows no evidence of developmental delay. Routine chromosome-banding analysis of the patient revealed an apparently balanced translocation between the long arm of chromosome 9 and chromosome 17: 46,XY, t(9;17)(q32;q12). His father and paternal grandmother had the same translocation seen in the patient; whereas, his mother had a normal karyotype (Fig. 1). Neither of the other translocation carriers had a cleft or malformations, and there was no family history of CL/P.

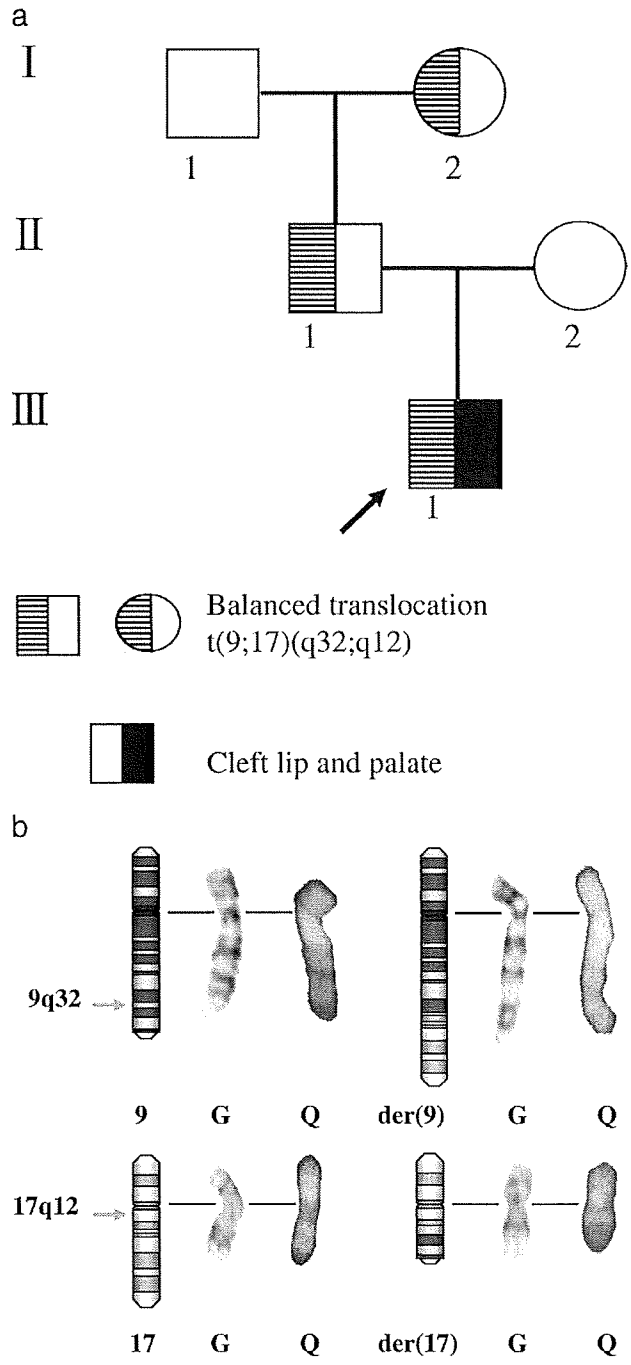

FIGURE 1 Case presentation. a: Pedigree of the family examined. b: Chromosomal breakpoints in the patient (III-1). Ideogram and a partial karyotype are shown. Chromosomal breakpoints are indicated by arrows.

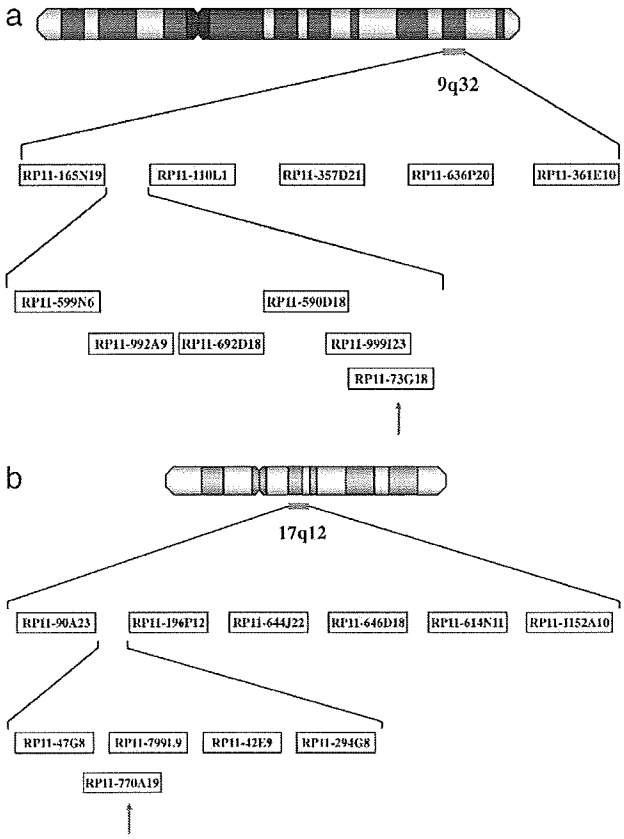

FIGURE 2 BAC clones used for FISH analysis. a: A physical map of BAC clones covering the 9q32 subchromosomal band. b: A physical map of BAC clones covering the 17q12 subchromosomal band.

Identification of Translocation Breakpoint

Fluorescence In Situ *Hybridization Analysis*

Breakpoint mapping of the translocation in the patient was initiated by FISH analysis, according to published procedures (Ono et al., 1997). Bacterial artificial chromosome (BAC) clones were identified using the genome maps provided by the National Center for Biotechnology Information (http://www.ncbi.nlm.org) and University of California, Santa Cruz (UCSC) (http://genome.cse.ucsc.edu) genome browsers. Figure 2 shows the BAC clones on chromosomes 9 and 17 used in the present study.

Cloning of the Translocation Breakpoint

We carried out a series of long-range PCR amplifications of DNA fragments to detect the recombinant sequence caused by the translocation. Primer sequences were designed based on the FISH results, with one forward primer on chromosome 9 and one reverse primer on chromosome 17, and were evaluated by RepeatMasker (http://www.repeatmasker.org/) to avoid nonspecific amplification of repetitive sequence. The PCR products then were subcloned into the pCR2.1-TOPO vector (Invitrogen, Carlsbad, CA). Additional nested primers were designed to obtain a DNA fragment including the breakpoint on der(9) using the subcloned plasmid DNA from the patient and genomic DNA of members of his family.

DNA Sequencing

The PCR products were labeled with the ABI PRISM BigDye Terminator Cycle Sequencing Ready Reaction Kit according to the manufacturer's instruction (Applied Biosystems, Carlsbad, CA). The products were purified, and then analyzed on an ABI 3700 automated sequencer (Applied Biosystems). The Applied Biosystems sequence software (version 2.1.2) was used for lane tracking. Chromatograms were transferred to a UNIX workstation, base-called with PHRED 4.0 (http://droog.mbt.washington.edu/poly_doc40.html) and results viewed with the CONSED program (version 4.0) (Nickerson et al., 1997). The UCSC and the Ensembl databases (http://www.ensembl.org) were used to detect potential genes around the breakpoint.

Mutation Search of Candidate Genes in Case/Control CL/P Population

To examine the association of the disrupted genes with the occurrence of CL/P in individuals unrelated to this family, we screened for mutations of the untranslated regions (UTR), exons and exon-intron boundaries of the two rearranged genes on chromosome 9 and chromosome 17. In addition, any plausible candidate gene adjacent to the breakpoint was screened. We sequenced 90 individuals affected with isolated CL/P from the Philippines and 90 from Iowa. The control group comprised 90 samples from unrelated Filipinos and whites provided by Centre d'Etudes du Polymorphisme Humaine (Dausset et al., 1990). Standard chi-square tests of association were used to compare the frequencies of each variant found by sequencing between groups of patients and controls.

Haplotype Analysis Adjacent to the Translocation Breakpoint

To determine whether the chromosomal regions adjacent to the breakpoint could play a role in the development of CL/P, we carried out the haplotype-based transmission disequilibrium test. Four tagging SNP markers (rs974230, rs1330691, rs4596714, rs3750534) adjacent to the breakpoint on chromosome 9 and three markers (rs16561, rs725276, rs1029719) on chromosome 17 were selected, based on the HapMap (http://www.hapmap.org/index.html.en) database. The TaqMan genotyping for these SNPs was performed with the ABI PRISM 7900 Sequence Detection System (Applied Biosystems) using 371 case/parent families from the Philippines and 206 from Iowa. Haplotype-based transmission disequilibrium statistics

were calculated using the software FBAT (Horvath et al., 2001; Rabinowitz and Laird, 2000).

Bioethics Approval

Committee approval was obtained from both the ethical committee at Toyohashi Municipal Hospital and Aichi-Gakuin University to obtain whole blood from the patient, his parents, and his paternal grandparents after signed informed consent. For the association analysis, patients were identified at the University of Iowa Hospital and Clinics and in the Philippines through Operation Smile (Murray et al., 1997). Blood samples were obtained with informed consent following institutional review board (IRB) approval in the United States (University of Iowa, IRB Committee) and in the Philippines (Hope Foundation, Bacolod City, Negros, Philippines).

Results

Identification of the Translocation Breakpoint

We found that two clones, RP11-73G18 (164,488 base pairs [bp]) and RP11-999I23 (160,162 bp), included the breakpoint region, judging from a hybridization pattern in which FISH signals were detected simultaneously on the normal chromosome 9 as well as both der(9) and der(17) chromosomes (Fig. 3a). The breakpoint on chromosome 17 was covered by two clones, RP11-770A19 (194,408 bp) and RP11-799L9 (178,732 bp), according to the hybridization pattern in which FISH signals were detected simultaneously on the normal chromosome 17 as well as both der(9) and der(17) chromosomes (Fig. 3b).

To examine sequences of the translocation breakpoints, we tried PCR amplification involving the breakpoint region (Fig. 4a). A primer set of F2 (5′-TCTTAACT-TACCTGTTGCTGCCGTTCCCTG-3′) derived from chromosome 9 and R1 (5′-TGGGCTGAGATTGTGG-TAACCGTAGGAAAG-3′) derived from chromosome 17 successfully amplified a DNA fragment of approximately 3 kbp in length. The PCR product amplified by 9f1 (5′-GTGTATGATACCATAACAATTAC-3′) and 17r1 (5′-GCACTGAGCAAACAGGAAGTG-3′) was sequenced after subcloning into the pCR2.1-TOPO vector. The nucleotide sequence of this PCR product demonstrated that the breakpoint of chromosome 9 lies in intron 1 of *SLC31A1* (solute carrier family 31 member 1; GenBank accession number NM001859, between nucleotides 113,072,186 and 113,072,187) according to the UCSC database (hg17). The breakpoint on chromosome 17 is assigned to the 5′UTR of chemokine ligand 2 (*CCL2*; GenBank accession number MN002982, between nucleotides 29,568,964 and 29,568,965). These three exons also form exons 4, 5, and 6 of a predicted six-exon gene of which *CCL2* may be one isoform, according to the Ensembl

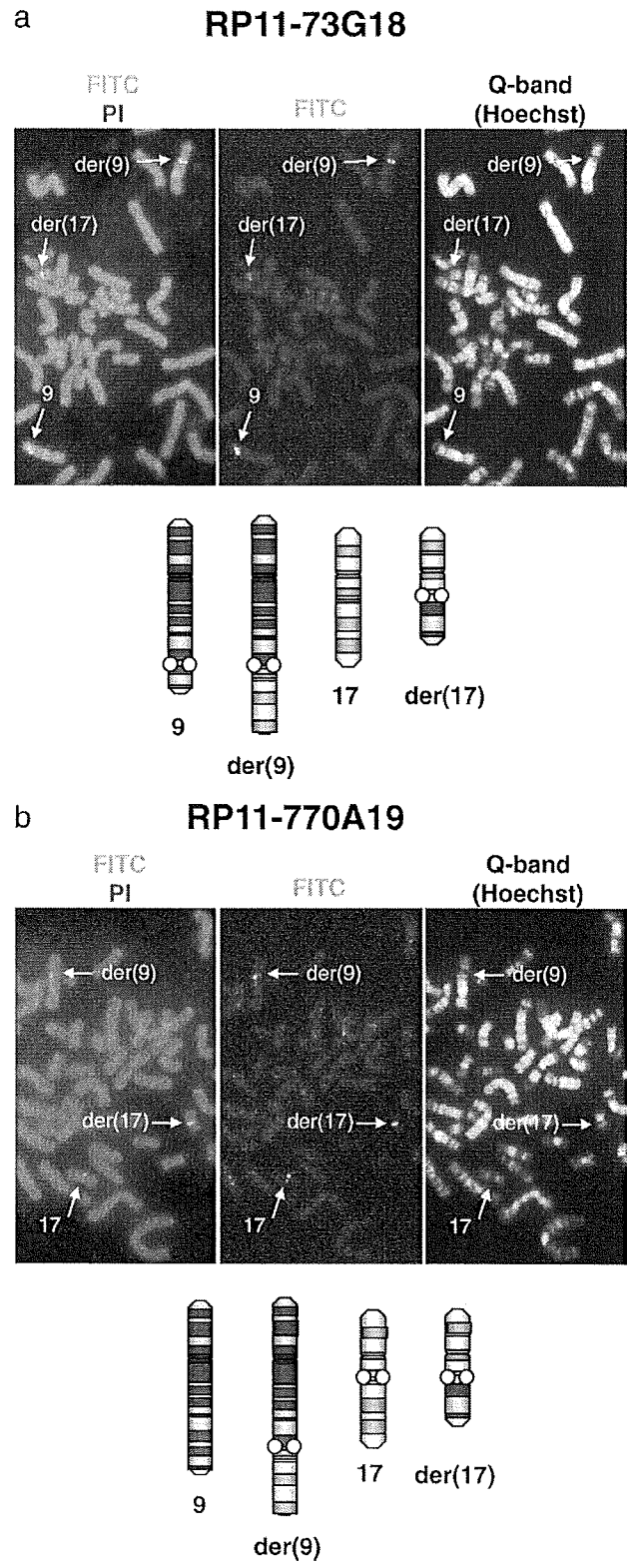

FIGURE 3 Molecular cytogenetic characterization of the t(9;17)(q32;q12). Each left panel shows FISH signals (FITC) on propidium iodide-stained chromosomes (PI). Each right panel exhibits Q-banded chromosomes (Hoechst). The RP11-73G18 clone simultaneously hybridized to normal 9, der(9), and der(17) chromosomes. The RP11-770A19 clone simultaneously hybridized to normal 17, der(9), and der(17) chromosomes. Bottom panels show schematic diagrams of FISH results.

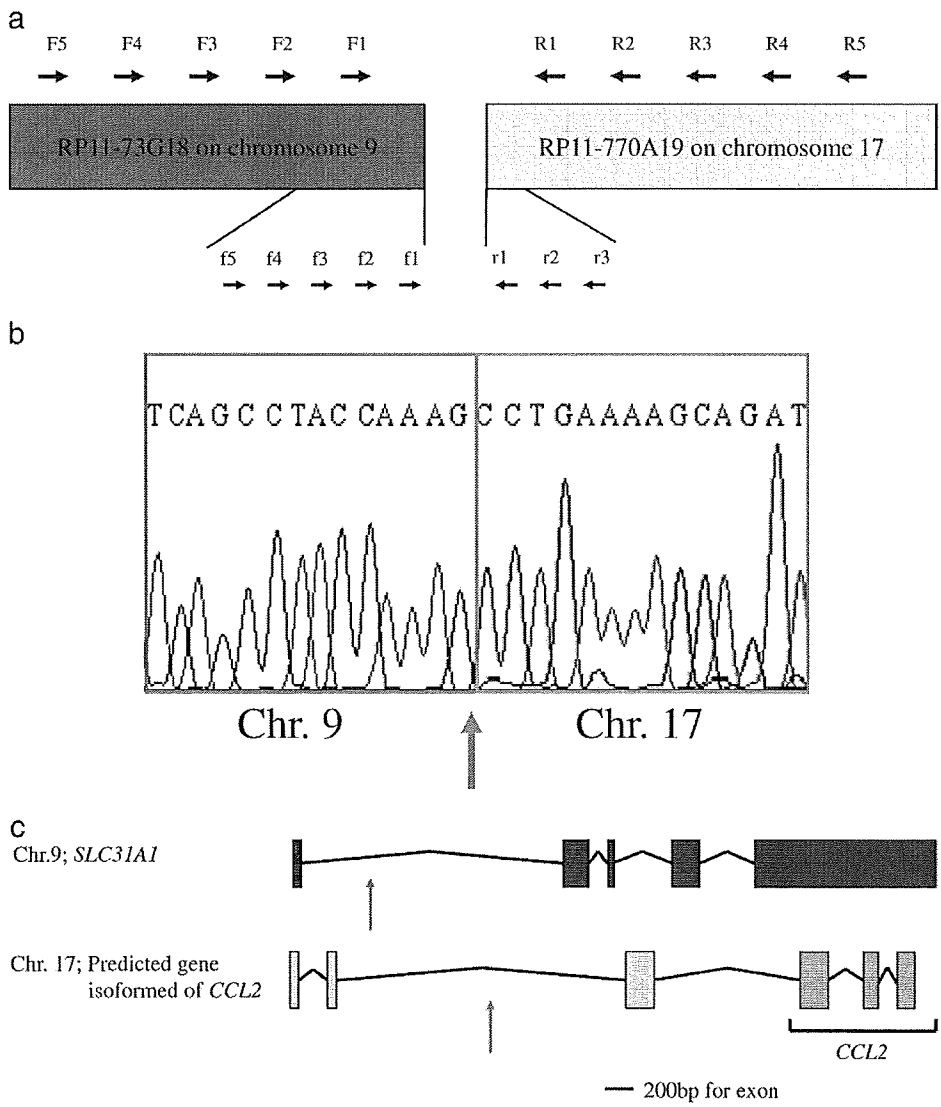

FIGURE 4 Fine mapping of the breakpoints. a: Primers used for long-range PCR. Forward and reverse primers were designed every 5 kbp of RP11-73G18 on chromosome 9 and RP11-770A19 on chromosome 17, respectively (arrows in upper). Additional primers flanked regions of the breakpoint (arrows in lower). b: Identification of the breakpoint on der(9), using a PCR product with a primer set of 9f1 and 17r1. c: The breakpoint on chromosome 9 is located between exons 1 and 2 of *SLC3A1*. The breakpoint on chromosome 17 is located between exons 2 and 3 of a predicted gene, according to the Ensembl database. Arrows indicate the positions of the breakpoints.

database (Transcript ID; GENSCAN00000016010). The function of this predicted gene is unknown. The translocation examined in this study shows no gain or loss of nucleotides at the breakpoint, confirming a perfectly balanced reciprocal translocation in translocation in the proband, his father, and his paternal grandmother (Fig. 4b and 4c).

Mutation Analysis of Candidate Genes in Case/Control CL/P Population

In order to determine whether genes at or near the breakpoint play a role in CL/P, we screened for mutations in three candidate genes: *SCL31A1* and *BSPRY* on chromosome 9 and the predicted gene that includes exons of *CCL2* on chromosome 17. Although *BSPRY* is located approximately 120 kbp downstream from the breakpoint, we considered it a plausible candidate because it is induced by the fibroblast growth factor receptor (*FGFR*) pathway (Welsh et al., 2007) and impaired FGF signaling has been found to be associated with 3% to 5% of CL/P (Riley et al., 2007). In addition, variants in a related gene, *SPRY2*, that also has a sprouty domain, already have been identified in CL/P (Vieira et al., 2005). We hypothesized that disruption of regulatory elements of *BSPRY* might lead to a cleft phenotype.

Table 1 shows nucleotide variants found in *BSPRY* and the predicted gene that include *CCL2*. In *BSPRY*, two

TABLE 1 Polymorphisms Found (Entries in the Table are Numbers of Individuals With Homozygous Common Allele/Heterozygous Rare Allele/Homozygous Rare Allele)

	Filipino Genotyping Distributions			*White Genotyping Distributions*			
Variant (Position)*	*Case (AF†)*	*Control (AF)*	*p Value*	*Case (AF)*	*Control (AF)*	*p Value*	*Comment*
BSPRY							
new (113202320)	62/0/0 (1.000)	68/5/0 (0.966)	.012	62/0/0 (1.000)	55/0/0 (1.000)	~.0	
rs752757 (113202508)	41/19/2 (0.814)	33/32/6 (0.690)	.058	55/22/2 (0.835)	25/7/1 (0.864)	0.756	
new (113202593)	49/2/0 (0.980)	65/3/0 (0.978)	.895	75/1/0 (0.993)	25/0/0 (1.000)	.449	
rs2296074 (113210279)	45/23/1 (0.819)	33/18/0 (0.825)	.565	42/4/0 (0.957)	33/6/0 (0.923)	.341	
Predicted gene (GENESCAN00000016010) containing *CCL2*							
rs4795884 (29527481)	52/32/6 (0.756)	42/36/1 (0.747)	.103	17/47/17 (0.500)	24/40/19 (0.530)	.396	
new (29527634)	82/0/0 (1.000)	79/0/0 (1.000)	~.0	74/6/0 (0.963)	57/4/0 (0.967)	.828	R15C‡
rs4795885 (29527655)	83/2/0 (0.988)	79/0/0 (1.000)	.103	53/23/3 (0.816)	38/20/3 (0.787)	.830	
new (29540781)	48/30/4 (0.768)	16/12/4 (0.688)	.364	60/19/3 (0.848)	53/25/2 (0.819)	.489	M33T‡
new (29540817)	79/6/0 (0.965)	69/0/0 (1.000)	.007	57/21/4 (0.823)	53/29/1 (0.813)	.198	N45S‡
new (29540841)	86/0/0 (1.000)	69/0/0 (1.000)	~.0	81/1/0 (0.994)	84/0/0 (1.000)	.234	T53M‡
new (29541048)	86/0/0 (1.000)	69/0/0 (1.000)	~.0	69/11/0 (0.931)	75/7/1 (0.981)	.290	
rs1860188 (29602669)	31/21/3 (0.755)	35/21/2 (0.784)	.833	49/12/2 (0.873)	22/13/0 (0.814)	.073	
new (29602875)	54/4/1 (0.949)	47/5/0 (0.952)	.463	63/0/0 (1.000)	73/0/0 (1.000)	~.0	
rs28730833 (29606607)	64/1/0 (0.992)	80/0/0 (1.000)	.204	56/0/0 (1.000)	80/0/0 (1.000)	~.0	
rs4586 (29607382)	10/19/8 (0.527)	11/27/14 (0.471)	.755	20/30/5 (0.636)	5/9/4 (0.528)	.363	

* Position according to UCSC database (hg17).
† AF = allele frequency.
‡ Amino acid change in predicted gene containing *CCL2* according to the Ensembl database (Transcript ID; GENSCAN00000016010).

common polymorphisms (rs752757 and rs2296074) and two new variants (positions 113202320 and 113202593) were detected. One variant (position 113202320) shows a significant p value (.012) in the Filipino CL/P population compared with matched controls. In the predicted gene containing *CCL2*, six new variants were detected. Four variants (positions 29527634, 29540781, 29540817, and 29540841) possibly result in a change of amino acid, R15C, M33T, N45S, and T53M, respectively, according to the Ensembl database (Transcript ID; GENSCAN-00000016010). R15C, N45S, and T53M were not found in Filipino controls, and T53M was not found in either Filipino or white controls. Five known variants were also identified (rs4795884, rs4795885, rs1860188, rs28730833, and rs4586). The variant at position 29540817 was present with a significant p value (.007) in an affected Filipino population compared with control population. No variants were identified in *SLC31A1* (data not shown).

Haplotype Analysis in Markers Adjacent to the Translocation Breakpoint

Although no statistically significant evidence of transmission distortion was seen for either SNP individually, there was statistically significant evidence of transmission distortion for haplotype h2-F9 (C-G-T-T; bi-allelic p value = .017) and haplotype h2-C9 (G-A-C-T; biallelic p value = .028) on chromosome 9 region (Table 2). We also confirmed statistically significant evidence for haplotype h5-F17 (G-G-T; biallelic p value = .042) and haplotype h8-F17 (G-A-A; biallelic p value = .017) on chromosome 17 region (Table 3). These p values, however, did not reach the level of significance, if we account for the number of tests done and use the conservative Bonferroni correction (0.0071).

Discussion

It has been demonstrated that CL/P is associated with trisomy 9q (Metzke-Heidemann et al., 2004), tetrasomy 9q (Wyandt et al., 2000), and chromosomal translocations involving the 9q region: t(6;9)(p23;q22.3) (Donnai et al., 1992); 46,XX,−22,+der(9)t(9;22)(q22;q11.2) (Pivnick et al., 1990); and 46,X,t(X;9)(p22.1;q32) (Zori et al., 1993). Naritomi et al. (1989) divided trisomy 9q syndrome into four groups (group 1: trisomy for 9q11>q32, group 2: 9q32>qter, group 3: 9q34, and group 4: 9q13/q21>qter) according to the length of the trisomic segment. Of these, the patients in groups 2 and 4 showed cleft palate, suggesting that the 9q32 segment may have important roles for facial development. Genome-wide linkage studies have revealed that the region 9q21 has significant linkage with facial clefting (Marazita et al., 2004). A number of candidate genes for CL/P in this region, 9q21–23, have been reported previously (*ROR2*, *PTCH*, *FOXE1*, and *TGFBR1*) (Ichikawa et al., 2006; Loeys et al., 2006; Mansilla et al., 2006; Mizuguchi et al., 2004; van Bokhoven et al., 2000; Vieira et al., 2005). Using a positional cloning approach, we demonstrated that *SLC31A1* on chromosome 9 was disrupted within its intron. The *SLC31A1* encodes a copper transporter and is itself not a strong candidate for involvement in facial development; although, unbalanced copper regulation can disturb cell metabolism (Lee et al., 2001). However, it is increasingly recognized that point mutations in regulatory elements located far from gene structural elements can be damaging. For example, mutations located up to ~1 Mbp from the gene *SHH* are capable of causing congenital abnormalities (Gurnett et al., 2007; Lettice et al., 2003) and campomelic dysplasia has resulted from a balanced translocation breakpoint 1.3 Mbp

TABLE 2 Results of Haplotype-based Transmission Disequilibrium Test for Single-Nucleotide Polymorphisms (SNPs) Around the Breakpoint on Chromosome 9

	SNP					
Filipino Haplotype	*a**	*b*	*c*	*d*	*Estimated Frequency*	*p Values (Biallelic)*
h1-F9	C	A	T	T	0.282	.456 (−)
h2-F9	C	G	T	T	0.246	.017 (+)
h3-F9	C	G	C	T	0.206	.095 (−)
h4-F9	C	A	T	C	0.053	.809 (+)
h5-F9	C	G	T	C	0.052	.892 (+)
h6-F9	G	A	T	T	0.047	.638 (−)
h7-F9	C	G	C	C	0.031	.093 (−)
h8-F9	G	G	C	T	0.027	.367 (+)
h9-F9	C	A	C	T	0.015	.594 (+)
h10-F9	G	G	T	T	0.013	.815 (+)
h11-F9	G	A	T	C	0.010	.956 (−)
h12-F9	G	G	C	C	0.010	.476 (+)
	SNP					
White Haplotype	*a*	*b*	*c*	*d*	*Estimated Frequency*	*p Values (Biallelic)*
h1-C9	G	A	T	T	0.137	.111 (−)
h2-C9	G	A	C	T	0.121	.028 (−)
h3-C9	G	A	T	C	0.110	.441 (+)
h4-C9	C	A	C	T	0.102	.342 (−)
h5-C9	G	A	C	C	0.087	.224 (+)
h6-C9	C	A	T	T	0.085	.122 (+)
h7-C9	G	G	T	C	0.065	.103 (+)
h8-C9	G	G	T	T	0.062	.624 (+)
h9-C9	G	G	C	T	0.059	.246 (+)
h10-C9	C	G	T	T	0.056	.198 (−)
h11-C9	C	G	C	T	0.039	.819 (+)

* a = rs1330692 C/G; b = rs3750534 A/G; c = rs4596714 C/T; d = rs974230 C/T.

downstream of the *SOX9* gene (Velagaleti et al., 2005). In the present report, although we did not detect any mutations in the *SLC31A1* gene itself, we did detect a significant *p* value for CL/P in the case-control study of a strong candidate for craniofacial development, the *BSPRY* gene, which is located 120 kbp downstream from the breakpoint (Table 1). Thus the translocation break may disrupt not the gene itself but regulatory regions. Moreover, there was significant evidence of transmission distortion for haplotypes on chromosome 9 (Table 2). In summary, it is possible that this region of chromosome 9q contains one or more genes playing a role in facial development.

TABLE 3 Results of Haplotype-Based Transmission Disequilibrium Test for Single-Nucleotide Polymorphisms (SNPs) Around the Breakpoint on Chromosome 17

	SNP				
Filipino Haplotype	*e**	*f*	*g*	*Estimated Frequency*	*p Values (Biallelic)*
h1-F17	A	G	T	0.322	.451 (+)
h2-F17	A	A	T	0.316	.991 (+)
h3-F17	A	A	A	0.103	.782 (+)
h4-F17	A	G	A	0.102	.973 (+)
h5-F17	G	G	T	0.065	.042 (−)
h6-F17	G	A	T	0.054	.450 (−)
h7-F17	G	G	A	0.025	.765 (−)
h8-F17	G	A	A	0.013	.017 (+)
	SNP				
White Haplotype	*e*	*f*	*g*	*Estimated Frequency*	*p Values (Biallelic)*
h1-C17	A	A	A	0.180	.275 (+)
h2-C17	A	A	T	0.164	.592 (+)
h3-C17	G	A	T	0.136	.597 (+)
h4-C17	G	A	A	0.120	.684 (−)
h5-C17	A	G	A	0.115	.899 (+)
h6-C17	G	G	T	0.112	.547 (−)
h7-C17	A	G	T	0.099	.534 (−)
h8-C17	G	G	A	0.075	.161 (−)

* e = rs16561 A/G; f = rs1029719 A/G; g = rs725276 A/T.

It is also possible that facial development may be influenced by genes on chromosome 17q. Case reports of chromosome translocations involving 17q24 (Czako et al., 2004; Luke et al., 1992), 17q25 (Bridge et al., 1985), 17q21.1 (Martinet et al., 2006), and 17q23.3 (Stalker et al., 2001) are associated with CL/P. Additively, genome-wide linkage analysis also shows significant association of the 17q21 region to the occurrence of CL/P (Marazita et al., 2004). Three candidate genes for CL/P in this region, 17q23–25, have been described (*SEPT9*, *MKS1*, and *GAA*) (Huie et al., 1999; Jeannet et al., 2001; Paavola et al., 1995). In addition, *RARA*, which is located approximately 6 Mbp downstream from the breakpoint studied here, is associated with CL/P (Chenevix-Trench et al., 1992). In this study we identified a predicted gene containing *CCL2* in the 17q breakpoint region. *CCL2* (monocyte chemotactic protein-1) is a member of the small inducible gene family and plays a role in the recruitment of monocytes to sites of injury and infection and so is not an obvious candidate for CL/P. We did, however, observe multiple amino acid variants in the predicted gene. One of them, a heterozygous variant in position 29540817 (possibly N45S), showed a significant p value in the Filipino CL/P population compared with the control population (Table 1). Moreover, there was statistically significant evidence of transmission distortion for two haplotypes on chromosome 17 in Filipinos but not in the white population (Table 3). These data suggest that the participation of this region in facial development may vary among different populations, and these results warrant an extension of these studies to larger numbers for confirmation.

Although three generations were examined here segregating the same chromosome translocation, only one individual was clearly affected with cleft lip and palate. CL/P is commonly nonpenetrant even in disorders caused by single gene mutations. Mutations in *IRF6* cause the autosomal dominant van der Woude syndrome, but there is only 70% penetrance for the CL/P phenotype (Burdick, 1986; Zucchero et al., 2004). Mutations in *MSX1* and several of the FGF and FGFR genes may also cause CL/P, but again only a subset of individuals with the mutation have a cleft phenotype (van den Boogaard et al., 2000). Isolated clefts are complex traits, not single-gene Mendelian disorders. They are likely caused by several interacting genes, each with small effects. In our case, the presumed loss of 50% of gene product may be the tipping point in an individual already having several other of the predisposing alleles/genes that may be absent in other family members with the translocation, hence their unaffected status. Clearly, future work is required to develop a better understanding of penetrance in CL/P.

In summary, we report an extensive study of candidate genes for CL/P based on a family with CL/P and segregating a balanced chromosome translocation t(9;17)(q32;q12). Analysis of the translocation shows disruption of *SLC31A1* on chromosome 9 and a predicted gene that includes *CCL2* on chromosome 17. It is intriguing that *SLC31A1* lies close to *BSPRY*, an excellent candidate gene for CL/P, and the results of a case-control study support a role for *BSPRY* in CL/P. In the aggregate, these data may provide additional support for an intensive search for genes/mutations and also for microdeletions in the 9q/17q region that would play a role in CL/P.

Acknowledgments. We are especially grateful to this family, many affected subjects, and their family members for their willingness to participate in this study. We thank Marla Johnson, Susie McConnell, and Adela Mansilla (University of Iowa) for technical assistance; and Qing Ying Li, Chiaki Nakagawa, Kyoko Takeshima, and Reiko Kimura (Aichi Human Service Center) for assistance in chromosomal analysis. We also thank Tadashi Yamamoto and Atsuo Kaetsu (Toyohashi Municipal Hospital) for clinical support.

References

Alkuraya FS, Saadi I, Lund JJ, Turbe-Doan A, Morton CC, Maas RL. SUMO1 haploinsufficiency leads to cleft lip and palate. *Science.* 2006;313:1751.

Blanton SH, Cortez A, Stal S, Mulliken JB, Finnell RH, Hecht JT. Variation in IRF6 contributes to nonsyndromic cleft lip and palate. *Am J Med Genet A.* 2005;137:259–262.

Bridge J, Sanger W, Mosher G, Buehler B, Hearty C, Olney A, Fordyce R. Partial duplication of distal 17q. *Am J Med Genet.* 1985;22:229–235.

Burdick AB. Genetic epidemiology and control of genetic expression in van der Woude syndrome. *J Craniofac Genet Dev Biol.* 1986;Suppl 2:99–105.

Chenevix-Trench G, Jones K, Green AC, Duffy DL, Martin NG. Cleft lip with or without cleft palate: associations with transforming growth factor alpha and retinoic acid receptor loci. *Am J Hum Genet.* 1992;51:1377–1385.

Czako M, Riegel M, Morava E, Bajnoczky K, Kosztolanyi G. Opitz "C" trigonocephaly-like syndrome in a patient with terminal deletion of 2p and partial duplication of 17q. *Am J Med Genet A.* 2004;131:310–312.

Dausset J, Cann H, Cohen D, Lathrop M, Lalouel JM, White R. Centre d'Etude du Polymorphisme Humain (CEPH): collaborative genetic mapping of the human genome. *Genomics.* 1990;6:575–577.

Donnai D, Heather LJ, Sinclair P, Thakker Y, Scambler PJ, Dixon MJ. Association of autosomal dominant cleft lip and palate and translocation 6p23;9q22.3. *Clin Dysmorphol.* 1992;1:89–97.

FitzPatrick DR, Carr IM, McLaren L, Leek JP, Wightman P, Williamson K, Gautier P, McGill N, Hayward C, Firth H, et al. Identification of SATB2 as the cleft palate gene on 2q32–q33. *Hum Mol Genet.* 2003;12:2491–2501.

Ghassibe M, Bayet B, Revencu N, Verellen-Dumoulin C, Gillerot Y, Vanwijck R, Vikkula M. Interferon regulatory factor-6: a gene predisposing to isolated cleft lip with or without cleft palate in the Belgian population. *Eur J Hum Genet.* 2005;13:1239–1242.

Gurnett CA, Bowcock AM, Dietz FR, Morcuende JA, Murray JC, Dobbs MB. Two novel point mutations in the long-range SHH enhancer in three families with triphalangeal thumb and preaxial polydactyly. *Am J Med Genet A.* 2007;143:27–32.

Horvath S, Xu X, Laird NM. The family based association test method: strategies for studying general genotype-phenotype associations. *Eur J Hum Genet.* 2001;9:301–306.

Huie ML, Kasper JS, Arn PH, Greenberg CR, Hirschhorn R. Increased occurrence of cleft lip in glycogen storage disease type II (GSDII): exclusion of a contiguous gene syndrome in two patients by presence of intragenic mutations including a novel nonsense mutation Gln58Stop. *Am J Med Genet.* 1999;85:5–8.

Ichikawa E, Watanabe A, Nakano Y, Akita S, Hirano A, Kinoshita A, Kondo S, Kishino T, Uchiyama T, Niikawa N, et al. PAX9 and

TGFB3 are linked to susceptibility to nonsyndromic cleft lip with or without cleft palate in the Japanese: population-based and family-based candidate gene analyses. *J Hum Genet.* 2006;51:38–46.

Jeannet PY, Watts GD, Bird TD, Chance PF. Craniofacial and cutaneous findings expand the phenotype of hereditary neuralgic amyotrophy. *Neurology.* 2001;57:1963–1968.

Jezewski PA, Vieira AR, Nishimura C, Ludwig B, Johnson M, O'Brien SE, Daack-Hirsch S, Schultz RE, Weber A, Nepomucena B, et al. Complete sequencing shows a role for MSX1 in non-syndromic cleft lip and palate. *J Med Genet.* 2003;40:399–407.

Kim HG, Herrick SR, Lemyre E, Kishikawa S, Salisz JA, Seminara S, MacDonald ME, Bruns GA, Morton CC, Quade BJ, et al. Hypogonadotropic hypogonadism and cleft lip and palate caused by a balanced translocation producing haploinsufficiency for FGFR1. *J Med Genet.* 2005;42:666–672.

Lee J, Prohaska JR, Thiele DJ. Essential role for mammalian copper transporter Ctr1 in copper homeostasis and embryonic development. *Proc Natl Acad Sci U S A.* 2001;98:6842–6847.

Lettice LA, Heaney SJ, Purdie LA, Li L, de Beer P, Oostra BA, Goode D, Elgar G, Hill RE, de Graaff E. A long-range Shh enhancer regulates expression in the developing limb and fin and is associated with preaxial polydactyly. *Hum Mol Genet.* 2003;12:1725–1735.

Loeys BL, Schwarze U, Holm T, Callewaert BL, Thomas GH, Pannu H, De Backer JF, Oswald GL, Symoens S, Manouvrier S, et al. Aneurysm syndromes caused by mutations in the TGF-beta receptor. *N Engl J Med.* 2006;355:788–798.

Luke S, Bennett HS, Pitter JH, Verma RS. A new case of monosomy for 17q25—qter due to a maternal translocation [t(3;17)(p12;q24)]. *Ann Genet.* 1992;35:48–50..

Mansilla MA, Cooper ME, Goldstein T, Castilla EE, Lopez Camelo JS, Marazita ML, Murray JC. Contributions of PTCH gene variants to isolated cleft lip and palate. *Cleft Palate Craniofac J.* 2006;43:21–29.

Marazita ML, Murray JC, Lidral AC, Arcos-Burgos M, Cooper ME, Goldstein T, Maher BS, Daack-Hirsch S, Schultz R, Mansilla MA, et al. Meta-analysis of 13 genome scans reveals multiple cleft lip/palate genes with novel loci on 9q21 and 2q32–35. *Am J Hum Genet.* 2004;75:161–173.

Martinet D, Vial Y, Thonney F, Beckmann JS, Meagher-Villemure K, Unger S. Fetus with two identical reciprocal translocations: description of a rare complication of consanguinity. *Am J Med Genet A.* 2006;140:769–774.

Metzke-Heidemann S, Kuhling-von Kaisenberg H, Caliebe A, Janssen D, Jonat W, Grote W, von Kaisenberg CS. Phenotypical variation in cousins with the identical partial trisomy 9 (pter-q22.2) and 7 (q35-qter) at 16 and 23 weeks gestation. *Am J Med Genet A.* 2004;126: 197–203.

Mizuguchi T, Collod-Beroud G, Akiyama T, Abifadel M, Harada N, Morisaki T, Allard D, Varret M, Claustres M, Morisaki H, et al. Heterozygous TGFBR2 mutations in Marfan syndrome. *Nat Genet.* 2004;36:855–860.

Mossey P, Little J. Epidemiology of oral clefts: an international perspective. In: Wyszynski DF, ed. *Cleft Lip and Palate: From Origin to Treatment.* New York: Oxford University Press; 2002:127–157.

Murray JC. Gene/environment causes of cleft lip and/or palate. *Clin Genet.* 2002;61:248–256.

Murray JC, Daack-Hirsch S, Buetow KH, Munger R, Espina L, Paglinawan N, Villanueva E, Rary J, Magee K, Magee W. Clinical and epidemiologic studies of cleft lip and palate in the Philippines. *Cleft Palate Craniofac J.* 1997;34:7–10.

Naritomi K, Izumikawa Y, Goya Y, Gushiken M, Shiroma N, Hirayama K. Trisomy 9q3 syndrome: a case report and review of the literature. *Clin Genet.* 1989;35:293–298.

Nickerson DA, Tobe VO, Taylor SL. PolyPhred: automating the detection and genotyping of single nucleotide substitutions using fluorescence-based resequencing. *Nucleic Acids Res.* 1997;25: 2745–2751.

Ono T, Kawabe T, Sonta S, Okamoto T. Assignment of MARK3 alias KP78 to human chromosome band 14q32.3 by in situ hybridization. *Cytogenet Cell Genet.* 1997;79:101–102.

Paavola P, Salonen R, Weissenbach J, Peltonen L. The locus for Meckel syndrome with multiple congenital anomalies maps to chromosome 17q21–q24. *Nat Genet.* 1995;11:213–215.

Park JW, McIntosh I, Hetmanski JB, Jabs EW, Vander Kolk CA, Wu-Chou YH, Chen PK, Chong SS, Yeow V, Jee SH, et al. Association between IRF6 and nonsyndromic cleft lip with or without cleft palate in four populations. *Genet Med.* 2007;9:219–227.

Pivnick EK, Wilroy RS, Summitt JB, Tucker B, Herrod HG, Tharapel AT. Adjacent-2 disjunction of a maternal t(9;22) leading to duplication 9pter—22 and deficiency of 22pter—q11.2. *Am J Med Genet.* 1990; 37:92–96.

Rabinowitz D, Laird N. A unified approach to adjusting association tests for population admixture with arbitrary pedigree structure and arbitrary missing marker information. *Hum Hered.* 2000;50:211–223.

Riley BM, Mansilla MA, Ma J, Daack-Hirsch S, Maher BS, Raffensperger LM, Russo ET, Vieira AR, Dode C, Mohammadi M, et al. Impaired FGF signaling contributes to cleft lip and palate. *Proc Natl Acad Sci U S A.* 2007;104:4512–4517.

Scapoli L, Palmieri A, Martinelli M, Pezzetti F, Carinci P, Tognon M, Carinci F. Strong evidence of linkage disequilibrium between polymorphisms at the IRF6 locus and nonsyndromic cleft lip with or without cleft palate, in an Italian population. *Am J Hum Genet.* 2005;76:180–183.

Stalker HJ, Gray BA, Zori RT. Dominant transmission of a previously unidentified 13/17 translocation in a five-generation family with Robin cleft and other skeletal defects. *Am J Med Genet.* 2001;103:339–341.

van Bokhoven H, Celli J, Kayserili H, van Beusekom E, Balci S, Brussel W, Skovby F, Kerr B, Percin EF, Akarsu N, et al. Mutation of the gene encoding the ROR2 tyrosine kinase causes autosomal recessive Robinow syndrome. *Nat Genet.* 2000;25:423–426.

van den Boogaard MJ, Dorland M, Beemer FA, van Amstel HK. MSX1 mutation is associated with orofacial clefting and tooth agenesis in humans. *Nat Genet.* 2000;24:342–343.

Velagaleti GV, Bien-Willner GA, Northup JK, Lockhart LH, Hawkins JC, Jalal SM, Withers M, Lupski JR, Stankiewicz P. Position effects due to chromosome breakpoints that map approximately 900 Kb upstream and approximately 1.3 Mb downstream of SOX9 in two patients with campomelic dysplasia. *Am J Hum Genet.* 2005;76: 652–662.

Vieira AR, Avila JR, Daack-Hirsch S, Dragan E, Felix TM, Rahimov F, Harrington J, Schultz RR, Watanabe Y, Johnson M, et al. Medical sequencing of candidate genes for nonsyndromic cleft lip and palate. *PLoS Genet.* 2005;1:e64.

Welsh IC, Hagge-Greenberg A, O'Brien TP. A dosage-dependent role for Spry2 in growth and patterning during palate development. *Mech Dev.* 2007;124:746–761.

Wyandt HE, Lebo RV, Fenerci EY, Sadhu DN, Milunsky JM. Tandem duplication/deletion in a maternally derived chromosome 9 supernumerary derivative resulting in 9p trisomy and partial 9q tetrasomy. *Am J Med Genet.* 2000;93:305–312.

Yoshiura K, Machida J, Daack-Hirsch S, Patil SR, Ashworth LK, Hecht JT, Murray JC. Characterization of a novel gene disrupted by a balanced chromosomal translocation t(2;19)(q11.2;q13.3) in a family with cleft lip and palate. *Genomics.* 1998;54:231–240.

Zori RT, Gray BA, Bent-Williams A, Driscoll DJ, Williams CA, Zackowski JL. Preaxial acrofacial dysostosis (Nager syndrome) associated with an inherited and apparently balanced X;9 translocation: prenatal and postnatal late replication studies. *Am J Med Genet.* 1993;46:379–383.

Zucchero TM, Cooper ME, Maher BS, Daack-Hirsch S, Nepomuceno B, Ribeiro L, Caprau D, Christensen K, Suzuki Y, Machida J, et al. Interferon regulatory factor 6 (IRF6) gene variants and the risk of isolated cleft lip or palate. *N Eng J Med.* 2004;351:769–780.

Search for Genomic Alterations in Monozygotic Twins Discordant for Cleft Lip and/or Palate

Jane W. Kimani,[1*] Koh-ichiro Yoshiura,[2] Min Shi,[3] Astanand Jugessur,[4] Danilo Moretti-Ferreira,[5] Kaare Christensen,[6] and Jeffrey C. Murray[1]

[1] Department of Pediatrics, University of Iowa, United States of America
(*currently at Department of Pathology and Lab Medicine, University of North Carolina, United States of America)
[2] Department of Human Genetics, Nagasaki University Graduate School of Biomedical sciences, Nagasaki, Japan
[3] Biostatistics Branch, National Institute of Environmental Health Sciences (NIEHS), United States of America
[4] Craniofacial Development, Murdoch Children's Research Institute, Royal Children's Hospital, Melbourne, Australia
[5] Servico de Aconselhamento, Genetico da Universidade Estadual Paulista, Botucatu, Brazil
[6] Department of Epidemiology, Institute of Public Health, University of Southern Denmark, Denmark

Phenotypically discordant monozygotic twins offer the possibility of gene discovery through delineation of molecular abnormalities in one member of the twin pair. One proposed mechanism of discordance is postzygotically occurring genomic alterations resulting from mitotic recombination and other somatic changes. Detection of altered genomic fragments can reveal candidate gene loci that can be verified through additional analyses. We investigated this hypothesis using array comparative genomic hybridization; the 50K and 250K Affymetrix GeneChip® SNP arrays and an Illumina custom array consisting of 1,536 SNPs, to scan for genomic alterations in a sample of monozygotic twin pairs with discordant cleft lip and/or palate phenotypes. Paired analysis for deletions, amplifications and loss of heterozygosity, along with sequence verification of SNPs with discordant genotype calls did not reveal any genomic discordance between twin pairs in lymphocyte DNA samples. Our results demonstrate that postzygotic genomic alterations are not a common cause of monozygotic twin discordance for isolated cleft lip and/or palate. However, rare or balanced genomic alterations, tissue-specific events and small aberrations beyond the detection level of our experimental approach cannot be ruled out. The stability of genomes we observed in our study samples also suggests that detection of discordant events in other monozygotic twin pairs would be remarkable and of potential disease significance.

Keywords: monozygotic twins, discordant, cleft lip and palate, genome-wide

Classical twin research studies comparing disease concordance rates between monozygotic (MZ) and dizygotic (DZ) twins have been extensively applied to estimate the contribution of genetic and environmental factors to many complex traits (Boomsma et al., 2002). MZ twin concordance for common diseases and traits rarely reaches 100%, an observation that is often attributed to differential environmental exposures (Wong et al., 2005). However, there are several molecular mechanisms that could underlie phenotypic discordance between MZ twins, such as *de novo* somatic mutations (Kondo et al., 2002), chromosomal anomalies (Gilbert et al., 2002), skewed X chromosome inactivation (De Gregorio et al., 2005), imprinting defects (Weksberg et al., 2002) and differential gene expression (Mak et al., 2004). The identification of molecular genetic differences between discordant MZ twins suggests that the utility of twin studies could be extended beyond heritability studies to gene discovery.

Postzygotic mitotic recombination and other somatic events such as deletions, nondisjunction, gene conversion, mobile genetic elements, fragile sites and repeat expansions have been proposed as a cause of MZ twin discordance (Cote & Gyftodimou, 1991; Kastern & Kryspin-Sorensen, 1988). Occurrence of somatic genomic changes in the early embryo can have significant implications for the phenotypes of the twins and the twinning process. If a genomic alteration occurs prior to twinning, unequal allocation of cells with the lesion to the two embryos could account for discordant phenotypes, with evidence of mosaicism, while the segregation of two genetically different populations of cells may trigger the twinning process, resulting in co-twins with discordant phenotypes (Machin, 1996). Since detection of chromosomal abnormalities relies on the comparison of a test genome with a reference genome sequence, the identical genomes of MZ twins ensure that any genomic differences can be established with confidence and

Received 11 November, 2008; accepted 17 June, 2009.

Address for correspondence: Jeffrey C. Murray, MD, University of Iowa, Department of Pediatrics, S. Grand Avenue, 2182 ML, Iowa City IA 52242 USA. E-mail: jeff-murray@uiowa.edu